ARL 63-157

DETONATION AND SHOCK-TUBE STUDIES OF HYDRAZINE AND NITROUS OXIDE

A. JOST
K. W. MICHEL
J. TROE
H. Gg. WAGNER

UNIVERSITY OF GOTTINGEN
GOTTINGEN, GERMANY

SEPTEMBER 1963

AEROSPACE RESEARCH LABORATORIES
OFFICE OF AEROSPACE RESEARCH
UNITED STATES AIR FORCE

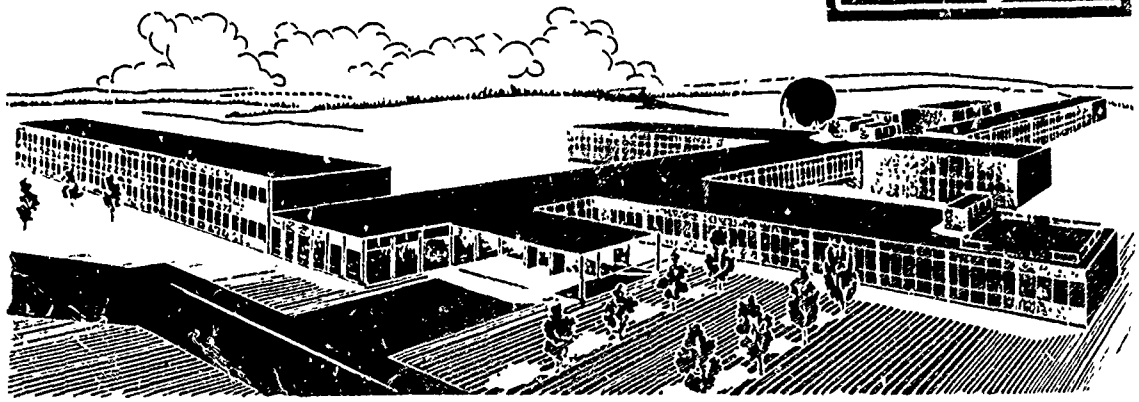

NOTICES

When Government drawings, specifications, or other data are used for any purpose other than in connection with a definitely related Government procurement operation, the United States Government thereby incurs no responsibility nor any obligation whatsoever; and the fact that the Government may have formulated, furnished, or in any way supplied the said drawings, specifications, or other data, is not to be regarded by implication or otherwise as in any manner licensing the holder or any other person or corporation, or conveying any rights or permission to manufacture, use, or sell any patented invention that may in any way be related thereto.

- - - - - - - - - -

Qualified requesters may obtain copies of this report from the Defense Documentation Center, (DDC), Cameron Station, Alexandria, Virginia.

- - - - - - - - - -

This report has been released to the Office of Technical Services, U.S. Department of Commerce, Washington 25, D.C. for sale to the general public.

- - - - - - - - - -

Copies of ARL Technical Documentary Reports should not be returned to Aerospace Research Laboratories unless return is required by security considerations, contractural obligations or notices on a specified document.

300 - October 1963 - 8-130-162

ARL 63-157

DETONATION AND SHOCK-TUBE STUDIES OF HYDRAZINE AND NITROUS OXIDE

A. JOST
K. W. MICHEL
J. TROE
H. Gg. WAGNER

UNIVERSITY OF GOTTINGEN
GOTTINGEN, GERMANY

SEPTEMBER 1963

Contract AF 61(514)-1142
Project 7013
Task 7013-01

AEROSPACE RESEARCH LABORATORIES
OFFICE OF AEROSPACE RESEARCH
UNITED STATES AIR FORCE
WRIGHT-PATTERSON AIR FORCE BASE, OHIO

FOREWORD

This report was prepared for the Aerospace Research Laboratories of the Office of Aerospace Research at Wright-Patterson Air Force Base, Ohio, by the Institute of Physical Chemistry at the University of Göttingen in Germany under Air Force Contract No. AF 61(514)-1142, Project No. 7013, "Research in Chemical Energetics", Task No. 701301, "Research on Energetic Processes in Gases". The project director at the University of Göttingen was Professor W. Jost, Head of the Institute of Physical Chemistry. Karl Scheller served as technical administrator for the Aerospace Research Laboratories. The report reviews the research performed during the period 1 March 1962 - 28 February 1963.

ABSTRACT

In continuing studies of kinetic and detonative properties of simple compounds, which contain nitrogen, experiments investigating the detonability of hydrazine - nitrous oxide mixtures are reported. No detonations could be produced in mixtures containing less than 7 vol.% of N_2O. Pure hydrazine shows a detonation velocity of about 2450 m/sec, which is close to the theoretical value calculated on the assumption of chemical equilibrium in the CHAPMAN-JOUGUET region. The measured velocities meet some of the criteria for stable detonations.

Spectroscopic investigations of the wake behind N_2H_4 detonations, however, revealed great amounts of ammonia which had not yet disappeared 300 μsec behind the detonation front. Such quantities of NH_3 and this long a reaction zone is not in accord with the measured velocity of the detonation. Some evidence based on the pressure dependence in the NH_3 production suggests that these detonations are inherently unstable.

In compiling data for the understanding of the kinetic aspects of the above detonations, shock-tube studies of the pyrolysis of nitrous oxide and hydrazine have been continued. Absorption coefficients od N_2O up to 1800 ^oK have been measured. In the temperature interval from 1530 ^oK to 1820 ^oK and at total gas densities of $1.5 \cdot 10^{-4}$ mole/cm^3 (6 atm.) the initial decomposition rate of N_2O mixed with an excess of Ar is given by the rate law $k_1 = 10^{10.8} \cdot \exp(-60\,000/RT)$ sec^{-1}. This is in agreement with results from measurements of the unimolecular decomposition rate at low temperatures. The second-order dependence of k_1 upon total

gas density suggests that this unimolecular reaction is determined by collicional activation under the present conditions. Photoelectric techniques are outlined which will allow the amount of nitric oxide formed in this reaction to be determined. Registration of the emission indicated the presence of the reaction $NO + O \longrightarrow NO_2^* \longrightarrow NO_2 + h\nu$, even at the comparatively high pressures of these experiments.

Measurements of the decomposition rate of hydrazine behind reflected shock waves with an excess of He have been extended up to temperatures of 1550 °K. Using He as a carrier gas reduces schlieren effects and facilitates the kinetic evaluation of short reaction periods, even though the shock-front curvature has to be accounted for. Extinction coefficients behind the incident shock waves were in agreement with those obtained in previous experiments with Ar. By appropriate evaluation of the half-lives it was established, that the rate of decomposition does not depend upon the nature of the carrier gas. Contrary to the results obtained in the temperature region between 1100 °K and 1400 °K, there was no distinguishable dependence of half-lives of hydrazine upon its partial density. The apparent energy of activation is not different than in the low temperature region, i.e. 40 kcal/mole.

Limitations of the present shock tube are indicated and a new tube, which has been constructed to meet more stringent requirements, is described.

TABLE OF CONTENTS

LIST OF ILLUSTRATIONS

LIST OF TABLES

SYMBOLS

CJ (subscript)	refers to Chapman-Jouguet state
ΔE	energy of reaction
D	detonation velocity
F (subscript)	refers to parameters in the shock front of a detonation
H	enthalpy
ΔH	enthalpy of reaction
I	recorded intensity of light
I_o	intensity of light without absorption in the gaseous phase
i (subscript)	refers to parameters at an intermediate stage of the reaction zone
k	rate constant of chemical reaction
M	Mach number
P	pressure
R	specific gas constant
s	slit width of monochromator
T	temperature
t	time
t_r	time interval between registration of detonation front and reflected shock wave
u	shock speed
u/u_1	attenuation of incident shock (per m)
u_5/u_1	velocity ratio of reflected and incident shock waves
x	geometric path length in absorption measurements
α	parameter representing amount of NH_3 formed behind detonations through hydrazine
β	parameter representing amount of NH_3 which has survived for a certain period of time in the wake of.

γ		ratio of specific heats
ε		decadic molar extinction coefficient
λ		wavelength
ρ		gas density
$\tau_{1/2}$		half-life of reacting molecules
ξ		degree of reaction
suscript	1	refers to initial gas in front of shock waves and detonations
"	2	refers to gas behind shock waves
"	5	refers to gas behind reflected shock waves

A. Studies of Detonations of Hydrazin-Nitrous Oxide Mixtures.

I. INTRODUCTION

Within this general program, in which the reaction behavior of hydrazine at elevated temperatures is investigated in the homogeneous gas phase, the interaction of hydrazine with various oxidizers is of both practical and theoretical concern. Flames supported by mixtures of hydrazine with oxygen, nitric oxide and nitrous oxide have been studied extensively in recent years (ref. 1-4). Some detailed investigations on the explosive combustion of hydrazine (ref. 5) have revealed several features peculiar to the oxidation of hydrazine. Studies of the detonability and reaction zone of detonations through hydrazine-oxidizer mixtures are expected to add some information to previous results.

The detonability of pure gaseous hydrazine at atmospheric pressure had been examined before (ref. 6). At that time, difficulties were met in combining hydrazine and nitric oxide or oxygen to form gaseous mixtures which were well defined at a pressure of 1 atm. Furthermore, it was shown that nitrogen dioxide could not be added to hydrazine at room temperature without immediate reaction (ref. 7). Nitrous oxide, on the other hand, can be saturated with hydrazine readily and the mixture is easy to deal with at temperatures below 70 °C, thus offering a convenient approach to studies of detonative combustion of hydrazine.

II. EXPERIMENTAL

A round aluminum tube was chosen for these detonation experiments with N_2H_4-N_2O mixtures. The test section had a length of 300 cm and a diameter of 8.4 cm (fig. 1). Three observation windows made of plexiglass were inserted 10 cm apart, the last one being 11 cm upstream from the end plate. All windows were mounted flush with the inner wall so that the gas flow was not disturbed. The whole tube was surrounded by an electric tape and could be heated uniformly.

The temperature of the test section had to be chosen according to the desired partial pressure of hydrazine, this being contingent upon condensation phenomena (ref. 6,8). At higher temperatures, hydrazine undergoes catalytic decomposition when in contact with metal and glass surfaces (cf. review in ref. 7). This would give rise to great uncertainties about the actual composition of the detonating gas mixtures. Hence, it was decided to restrict these measurements to initial temperatures of 43 °C (except for detonations with pure hydrazine vapor and mixtures containing 83 vol% hydrazine, where the temperature was 67 °C), entailing a partial pressure of hydrazine of less than 40 mm Hg. Total pressures of the test mixtures lay, in general, around 90 mm Hg in the reported series of measurements.

Detonations of mixtures with 7-30 vol% hydrazine in nitrous oxide, as well as of pure hydrazine, were initiated by hydrogen-oxygen detonations in a driver section 160 cm long and with the same diameter as the test section. Initiator gas and test mixtures were separated by an aluminum foil which ruptured

under the impact of the initial detonations.

The initial pressure in the initiator section was made high enough (450 mm Hg, viz. 5 times higher than the initial pressure of the test gas, cf. ref. 9, p. 356) so that detonations of the nitrous oxide-hydrazine mixtures could be initiated readily. The composition of the initiator was conveniently set by restricting the flow rates of hydrogen and oxygen with the aid of properly gauged capillaries before the partners were mixed and passed through the driver section. Flow velocities were controlled by means of capillary flow meters. Two different mixtures of the initiator gas were used, the one contained 40 $\pm$ 2 vol% H_2 the other one 60 vol% H_2 (balance O_2), providing calculated detonation velocities of D=2080 $\pm$ m/sec and D=2770 m/sec. The former value lay in the range expected for detonation velocities of the test mixtures considered.

The test mixtures with 70 vol% N_2O or more were prepared by passing nitrous oxide, after expansion to a lower pressure, twice through liquid hydrazine (fig. 1). Difficulties in saturating gases with hydrazine vapor have been reported before (ref. 6 and 7). Even though hydrazine evaporates sluggishly, it condenses readily. Thus, when leading partially saturated N_2O through a condenser, the temperature of which was kept approximately 10 °C below that of the saturator, the partial pressure of hydrazine in the gas flow could be calculated reliably on the basis of the condenser temperature.

The glass tube transforming the N_2O-N_2H_4 mixture to the test section, as well as the test section itself, were heated

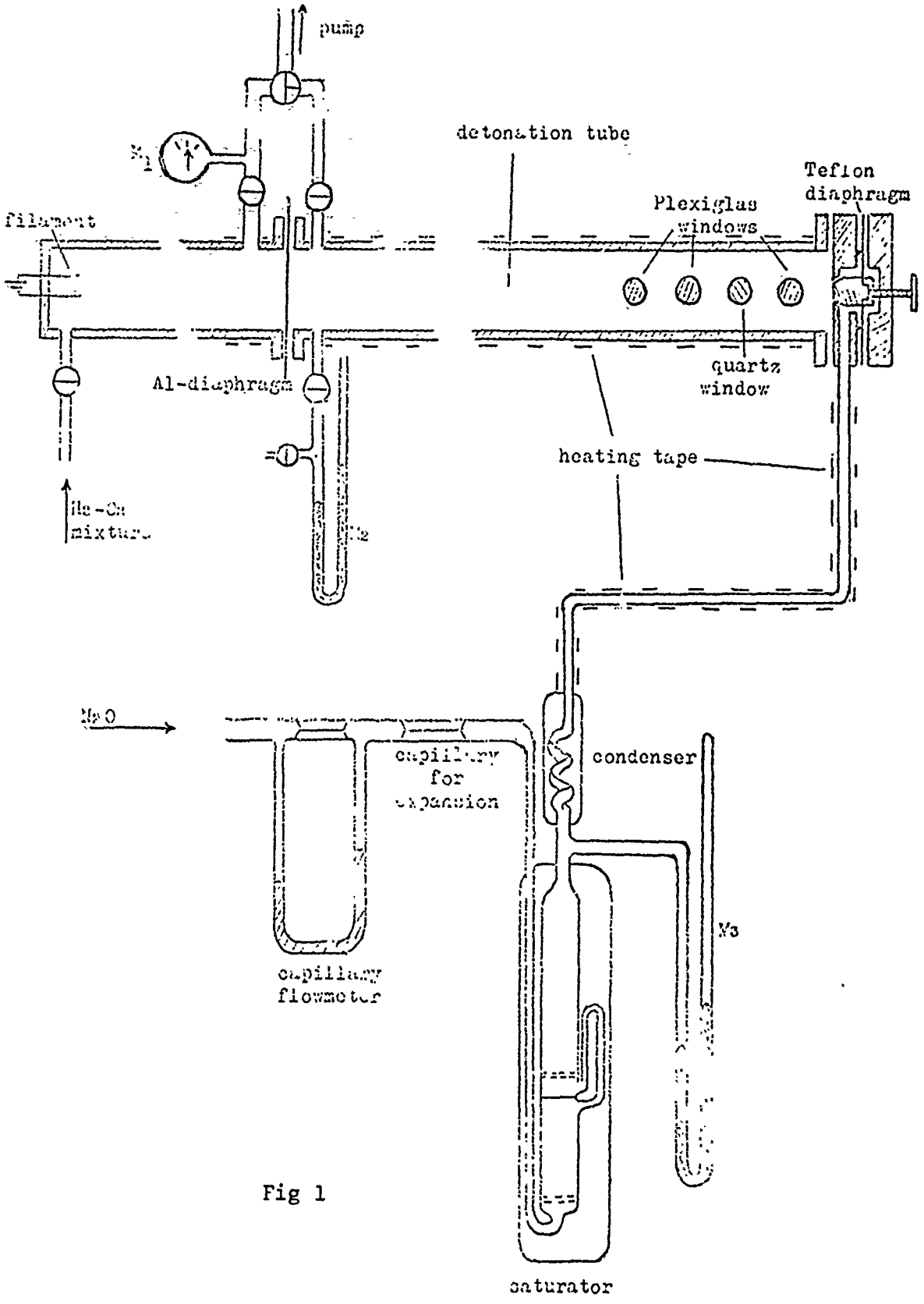
pump
detonation tube
Teflon diaphragm
Plexiglas windows
filament
Al-diaphragm
quartz window
heating tape
condenser
capillary for expansion
capillary flowmeter
saturator

Fig 1

appreciably above the condensation temperature of hydrazine. Still, previous experiments had shown (ref. 6 and 7) that adsorption of hydrazine at the tube wall might produce great deviations from the initial concentration of hydrazine. Therefore, the test section was swept a few times with the test mixture under the initial pressure of an experiment. The higher the partial pressure of hydrazine, the larger the amounts of gas were which had to be passed through the tube before the interfacial equilibrium was approached. In order to reach this point within a reasonable period of time, a special valve was constructed (see fig. 1 and fig. 21, p.58) which allowed adequate flow velocities (ca. 10 cm^3/sec STP and higher).

In general, the gas volume in the test section was replaced at least eight times before an experiment was started. Even though this method was suitable to gas mixtures containing lower concentrations of hydrazine, it quite evidently failed for mixtures with more than 30 % N_2H_4.

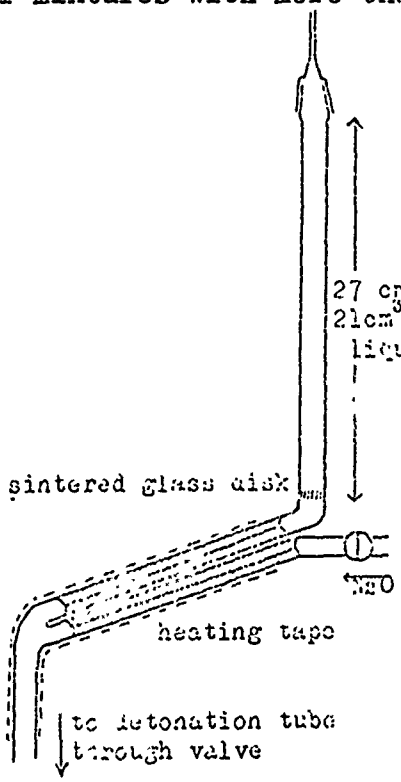

Fig. 2

In preparing test gas mixtures with 80-100 vol.% N_2H_4, another principle was used (fig. 2). Liquid hydrazine streamed at room temperature and atmospheric pressure from a graduated cylinder into a capillary which was heated to about 80 °C by a surrounding electric tape. Thus, the capillary served both as evaporator and flow regulator, viz. expansion nozzle down to a pressure of about 90 mm Hg. Beyond the capillary, the gaseous hydrazine could be mixed with nitrous oxide, which had been pre-

heated while streaming through another capillary. The flow velocity of hydrazine was controlled by timing the outflow from the graduated cylinder and was shown to be reasonably constant (ca. 5 millimole/sec). The method proved to be reliable and without risk. Before, each run the test section was thoroughly evacuated in order to remove water which had been formed as a reaction product of the previous experiment.

Prior to measuring the initial pressure of the test gas by means of a mercury manometer, which was at room temperature, some nitrogen was administered to manometer M_2 (fig. 1), thus, providing a gas cushion and preventing the condensation of hydrazine. The composition of the test gas was not affected by this procedure, because the pressure was set during the flushing of the tube.

The initiator gas was ignited by slowly increasing the current through a filament (fig. 1), to avoid premature triggering of the oscilloscope. The speed was measured with the aid of a conventional schlieren arrangement; three photomultipliers (ROA 931A) converted the light signals to electric pulses; the first schlieren spike triggered the oscilloscope sweep (Tektronix 545, 53/54 K plug-in unit). The electric time constant was calculated to be ca. 6 μsec.

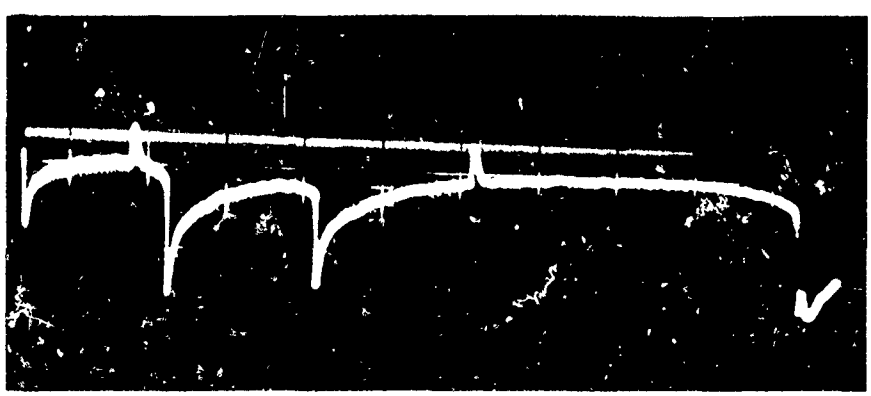

Fig 3

Fig. 3 shows a typical oscilloscope record. The positive pips are 100 μsec timing markers furnished by a Tektronix time-mark generator (Type 181, quartz-stabilized). The first schlieren-signal is clearly recorded on the screen. As the detonation front proceeds, greater and greater thermal radiation is recorded by the three photomultipliers and the photocurrent increases. The last abrupt change in photocurrent at the end of the trace is presumably caused by the strong light emission concomitant with the reflected shock. The detonation velocity could be measured with an accuracy of 0.5 %, after photographic enlargement of the oscilloscope records.

III. MATERIALS

Liquid anhydrous hydrazine, furnished by FLUKA AG, was employed without further purification. It contained less than 2 % water. Mass spectroscopic analysis indicated that the impurity level after evaporation was reduced to less than 0.1 %.

Nitrous oxide, anaesthetic grade, was provided by FARBWERKE HOECHST AG and was at least 98 % pure. Since these experiments were of exploratory nature, further purification by destillation was not mandatory.

The leak rate of the test section amounted to 10^{-3} mm Hg/min. Most of the air penetrated the flange holding the diaphragm. In any case, it was computed that the test gas could not contain more than 0.1 % air due to leaking.

RESULTS

Detonation velocities did not show any attenuation or acceleration within the range of accuracy of these experiments. Depending upon the composition of the mixture, theyranged from 1803 m/sec (7.7 vol% N_2H_4) to 2600 m/sec (83 vol% N_2H_4) at initial pressures of P_1 = 90 mm Hg and P_1 = 63 mm Hg (fig. 4). The initial temperature was 316 ^oK except for experiments with 83 and 100 vol% N_2H_4. Then the initial temperature had to be raised to T_1 = 340 ^oK in order to provide a sufficient high vapor pressure. A mixture of nitrous oxide with 7.7 vol% N_2H_4 still produced detonations.

For mixtures containing 7 vol% and 6 vol% N_2O as well as for pure nitrous oxide, however, only strongly attenuated shock waves were recorded. With pure nitrous oxide, these shock velocities averaged around 930 m/sec for initiator mixtures of $3O_2+2H_2$ and around 1210 m/sec for stoichiometric initiator mixtures (O_2+2H_2).

Detonation velocities of mixtures containing more than 7 vol% N_2O were faster by at least a factor of 2 than the above shock speeds. Within the accuracy of these determinations they did not show any attenuation or any dependence upon starting pressure (P_1 = 63 and 90 mm Hg) or composition of the initiator mixture. Nevertheless, strong fluctuations occur among the measured points (fig. 4). This might be due to inaccuracies in the test

gas composition. The effects of adsorption of hydrazine on the walls and heterogeneous decomposition have not been investigated in these experiments. In any case, the points indicate a definite trend in the concentration and show some of the characteristics of stable detonations. The behavior of pure nitrous oxide sufficiently demonstrates that the measured velocities do not result from overdriven detonations. The limits of detonability have not been established exactly, because the present detonation tube does not fulfil the requirements of such determinations (ref. 9. p. 338).

In some experiments, where the time constant of the electrical recording unit was properly selected, the rise time of the schlieren signals was found to be as long as 5 μsec. (this is in agreement with the rise time of absorption signals, see p. 16).

The experimental arrangement (width of ligth beam) does not account for more than 0.5 μsec. Thus, one might conclude that the detonation front is either strongly curved or tilted, a phenomenon which usually appears in detonation waves of inherent instability (cf. e.g. ref. 16).

V. CALCULATION OF DETONATION VELOCITIES

The theoretical values for detonation velocities have been calculated by iteration under the assumption discussed in the literature (cf. e.g. ref. 9). Enthalpies of reaction and specific heat data have been taken from ref. 10, energies for the various components were obtained from ref. 11. The following table shows the results of the computation for six different mixtures at starting pressures of 90 mm Hg, including the equilibrium

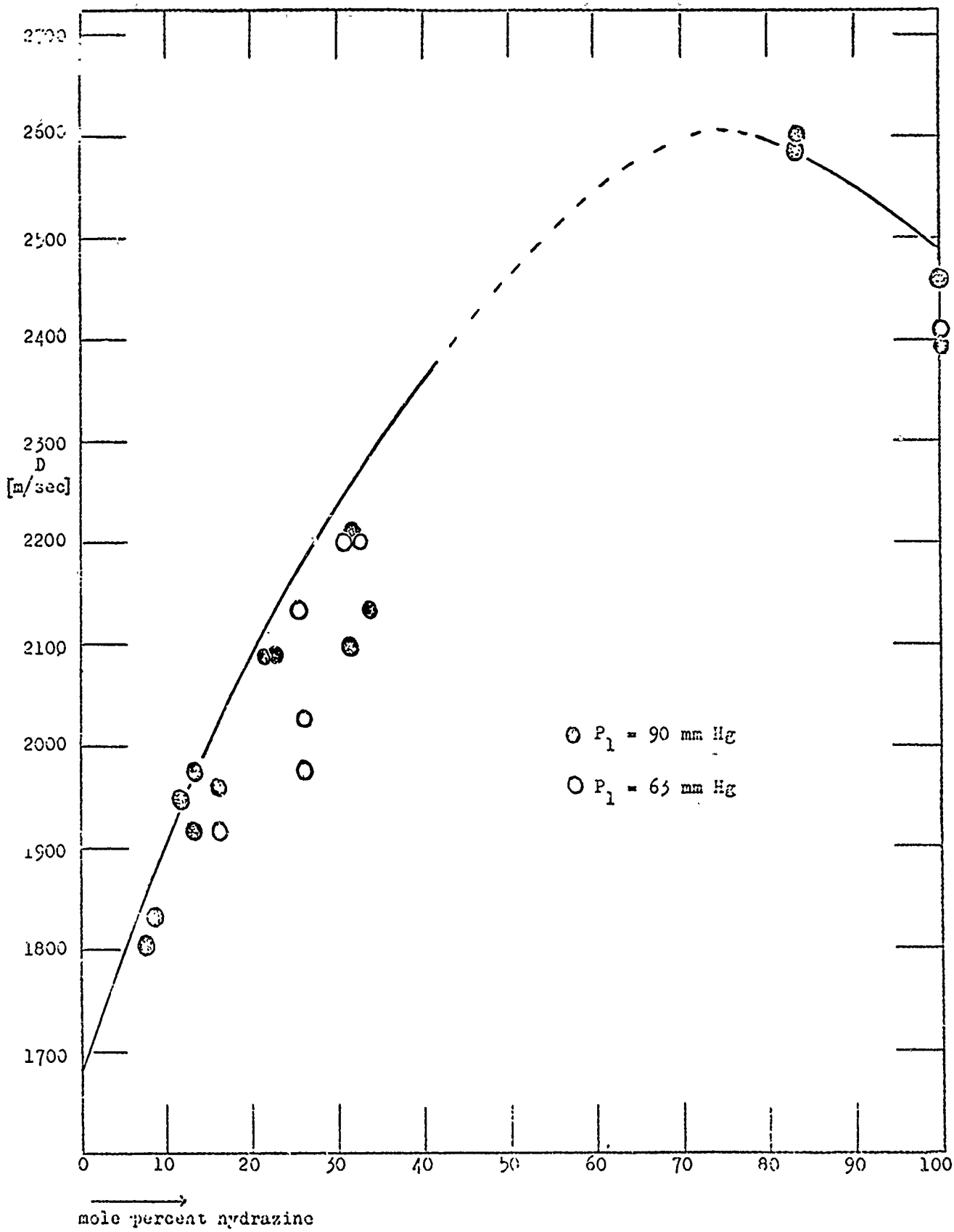

Fig. 4. Detonation Velocities of Nitrous Oxide - Hydrazine Mixtures

concentrations of the species NO, OH and O in the Chapman-Jouguet zone. Subscript F refers to conditions just behind the shock front, subscript C-J denotes parameters of the Chapman-Jouguet zone. In calculating the detonation velocity of pure hydrazine, it has been assumed that all of the hydrazine has been converted to nitrogen and hydrogen

$$N_2H_4 \longrightarrow 2\,H_2+N_2 \qquad \Delta E = -25.62 \text{ kcal/mole at } 340\ ^{\circ}K.$$

Table I

Computed Detonation Parameters

p_1 = 90 mm Hg.

% N_2H_4	T_1	T_F	$^{\circ}K(v_1/v_2)_F$	T_{C-J}	$^{\circ}K$ $(v_1/v_2)_{C-J}$	NO %	OH %	O %	D m/sec	M
0	316	1483	9.24	2555	1.740	2.94	-	0.62	1 683	6.11
10	316	1700	10.36	2995	1.756	4.14	3.46	2.83	1 983	6.86
20	316	1785	11.35	3228	1.764	3.48	5.79	3.75	2 089	7.43
33.3	316	1861	12.43	3337	1.769	1.85	5.62	2.68	2 275	7.97
80	340			2674	1.754	0.005	0.06	0.002	2 594	8.51
100	340	1427	18.15	1995	1.736	-	-	-	2 488	7.99

T_1 = Initial gas temperature

T_F = Temperature behind shock front

T_{C-J} = Temperature at Chapman-Jouguet zone

v_1/v_2 = Ratio of specific volumes

M = Mach numbers with respect to initial gas

The theoretical curve for the detonation velocities is included in fig. 4. The highest of the strongly scattering experimental points tend to be fairly close to the calculated

values, confirming again that actual detonation velocities have been measured. The downward trend of the average of all points indicated that uncontrolled effects have eventually decreased the hydrazine concentration of the gas phase.

VI. DISCUSSION

The purpose of these exploratory investigations was to outline experimental possibilities for future work and to check the methods to be applied. It was demonstrated that this approach holds promise of disclosing some interesting properties of the detonations of hydrazine-nitrous oxide mixtures as well as of pure hydrazine vapor. Evidently, there is a limit of detonability which lies fairly close to 100 vol.% N_2O, and which might show a strong dependence upon initial temperature. All attempts to produce detonations through pure nitrous oxide at initial temperatures of 316 ^{o}K and initial pressures of 90 mm Hg failed. Under these conditions a temperature of only 1480 ^{o}K was calculated for the front of virtual detonation (table I), a value much too low to induce a rapid enough decomposition of pure nitrous oxide. Some shock wave experiments reported by STREHLOW and COHEN (ref. 20) have indicated that, at a shock temperature of 1400 ^{o}K, adiabatic explosion of N_2O is preceded by an induction period of several hundred microseconds. In order to provide a higher temperature behind the detonation front, viz. a reaction zone short enough to facilitate self-supported detonations, one might raise the initial temperature of the test gas appreciably above the values applying in the reported experiments. This might be assumed in analogy to predictions concerning the decomposition flame of NO. These prediction were verified by preheating the

the gas to 900 °C (ref. 13). On the other hand even small additions of hydrazine might bring about a substantial change in the critical parameters for detonation. While studying the critical parameters in the inflammation of cyclohexane-nitrous oxide, Russian workers (ref. 14) found an unusually low threshold fuel concentration of 0.3 % C_6H_{12}. Similar effects seem to control N_2H_4-N_2O detonations.

The detonation velocity of pure hydrazine reveals an interesting feature: two values are conceivable for this case. Either the detonation velocitiy is determined by the composition of the reaction products, generally observed in the decomposition of hydrazine (ref. 7, 15):

$$N_2H_4 \longrightarrow NH_3 + 1/2\ N_2 + 1/2\ H_2 \quad \Delta H^0 = -34.8 \text{ kcal/mole } (T=340\ ^\circ K)$$

or by the equilibrium composition, which, because of the inertness of the intermediate product NH_3, can be attained only after a long reaction period:

$$N_2H_4 \longrightarrow N_2 + 2H_2 \qquad \Delta H^0 = -22.42 \text{ kcal/mole.}$$

The former case would yield a detonation velocity of 2200 m/sec and is definitively excluded by the present results. The detonation velocity given by chemical equilibrium in the Chapman-Jouguet plane, D = 2488 m/sec, is in close agreement with the experimental values. There is no good reason to assume that hydrazine decomposition in the reaction zone of a detonation occurs according to a different mechanism than in shock waves and flames. The actual processes which control the development of hydrazine detonations are visualized in different experiments (cf. section B).

B. Absorption Measurements in Detonations with Hydrazine

I. INTRODUCTION

Studies of detonation velocities of nitrous oxide-hydrazine mixtures seem to show that, in practically all cases, the composition of reaction products in the CHAPMAN-JOUGUET zone, which determines the detonation velocity, corresponds to chemical equilibrium. It is known, however, that in the temperature range under consideration and within the reaction periods available neither the pyrolysis of pure N_2O (qualitative detection of NO, see section C) nor that of N_2H_4 leads to an equilibrium composition of reaction products (ref. 7, 15). The thermal decomposition of hydrazine is comparatively well understood and a postulated normal chain mechanism is in good agreement with both the observed over-all rate and stoichiometry of the reaction which is $N_2H_4 \rightarrow NH_3 + 1/2\ N_2 + 1/2\ H_2$. Additionally, some data about the pyrolysis of the primary reaction product NH_3 have been reported in ref. 7. From this it can be derived that the thermal decomposition of NH_3, even in the wake of a detonation front, might proceed quite sluggishly.

Because more accurate data about the reaction behavior of hydrazine and ammonia are available at present, interest has been focussed upon processes governing the development of detonations with pure hydrazine. The measured detonation velocity demands that the over-all stoichiometry follows the equation $N_2H_4 \longrightarrow N_2 + 2H_2$. Kinetic evidence, on the other hand, suggests a fast conversion with ammonia as a major reaction product,

followed by the slow pyrolysis of NH_3. Such a slow consecutive reaction, however, would give rise to an unusually long reaction zone of an order of magnitude which has not been observed hitherto even at low pressures (ref. 9 p. 374, ref. 35 - 38). An alternative reaction path might include the direct conversion of hydrazine to nitrogen and hydrogen without the intermediate formation of ammonia. Since the species N_2H_4 and NH_3 possess absorption spectra in the ultraviolet, with roughly known temperature dependence (ref. 7), an available set-up for photoelectric recording could be used to decide to which degree the one or the other reaction path is preferred in the reaction zone of N_2H_4 detonations at low pressures.

II. METHODS

Monochromator and optical alignment with the detonation tube (section A) were as described in connection with previous shock-tube experiments (ref. 6,7). A UV light sheet passed through quartz windows, 21 cm upstream from the closed end. Absorption measurements were made mainly at a wavelength of 2500 Å with a monochromator slit width of about 0.34 mm (dispersion $d\lambda/ds \approx 36$ Å/mm). The effective beam width inside the tube amounted to 1.5 mm allowing a time resolution of 0.6 µsec behind the detonation front and 1.4 µsec for measurements behind the reflected wave (velocities of detonation and reflected wave 2.488 mm/µsec and 1.09 mm/µsec, resp.). The actual rise times of the absorption signals behind the fronts of the detonations and reflected shocks were 5 and 10 µsec, resp., indicating again strong curvature or tilt of the

corresponding surfaces (see fig. 5, the same result as with schlieren effects, cf. p 9.).

Calibration of the light intensity was made with a rotating sector of 2.8 kc/sec. In this case, however, the intensity recorded with the empty tube was not identical with the characteristic quantity I_0, on the basis of which the transmission change during an experiment is calculated. As the tube was filled with hydrazine vapor, a film of liquid hydrazine was deposited on the walls and also on the quartz windows. This film reduced the intensity of the incident light appreciably and was not affected by the detonations in the gas phase. Even when evacuating the tube, it evaporated only reluctantly, as shown by the slow regain of the full light intensity.

Hence, prior to an experiment and after the tube had been filled, the intensity of the transmitted light I_1 was measured. During experiments at starting pressures of P_1 = 90 mm Hg, practically all light absorbing species decomposed behind the reflected wave, so that the oscilloscope trace approached a level which was identified with the one corresponding to full light transmission I_0 without any absorption from the gaseous phase (cf. fig. 5a). The difference $I_0 - I_1$ could be read from the oscilloscope records and the molar absorption coefficient of hydrazine at 340 ^{o}K could be calculated. It was found to be $\varepsilon \cdot x = 1.0 \cdot 10^5$ cm^3/mole (x = geometric path length). Knowing the extinction coefficient of unreacted hydrazine, the value of I_1 and the gas pressure made it possible to derive the value of I_0 also for experiments which did not show full light transmission on the oscilloscope (fig. 5b - d).

The trigger to the oscilloscope was provided by one of the schlieren stations, described in section A. The detonation speed was examined on the basis of the time difference recorded between passage of the detonation and of the reflected wave through the UV light beam. Other details of the experimental procedure and of computing the reaction conditions have been mentioned in section A.

III. RESULTS

The oscilloscope records in fig. 5 illustrate the absorption traces behind detonations of hydrazine at four different starting pressures. The sweep speed was 50 μsec/cm, the vertical deflection 0.2 V/cm. The horizontal straight trace corresponds to the initial absorption through hydrazine. Upon arrival of the detonation front, the absorption increases. This, however, cannot be caused by undecomposed hydrazine. Table I (p.11) includes the temperature and density ratio for the shock front of a stable detonation through hydrazine. At a temperature of 1427 ^{o}K and a density of about 8.10^{-5} mole/cm^3, the expression for the half-lives (ref. 15) $\tau_{1/2} \approx \rho^{-1/2}.10^{-14.4}.\exp(+40000/RT)$ sec. suggests, that most of the hydrazine has been decomposed within less than 1 μsec under isothermal conditions and the more so when thermal self-acceleration by adiabatic heat release takes place. Moreover, due to the time compression effect this reaction time appears to the observer to be shortened by a factor which varies between 18 and 3. (In order to transform observed reaction time to a particle time scale, the former has to be multiplied by the density ratio with respect to the initial gas. This density ratio varies across the reaction zone as illustrated by fig. 6).

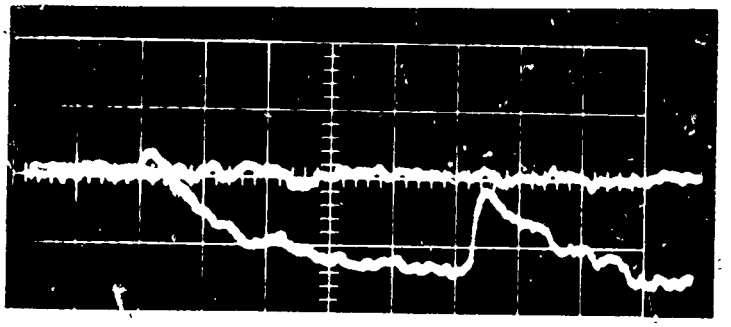

a) P_1=90mmHg

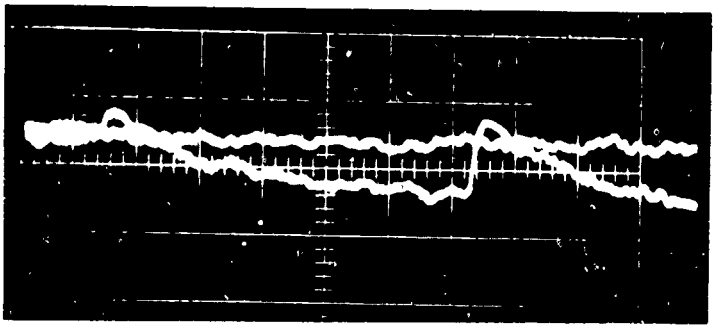

b) P_1=60mmHg

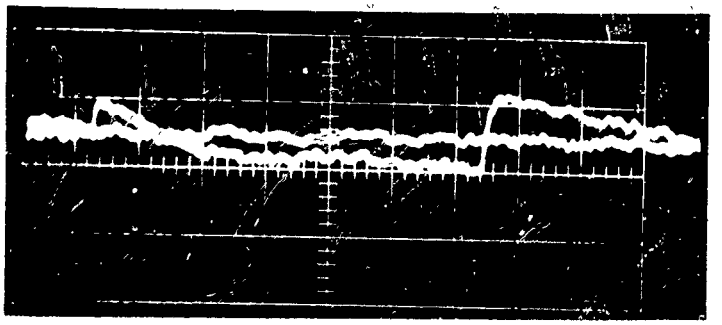

c) P_1=40mmHg

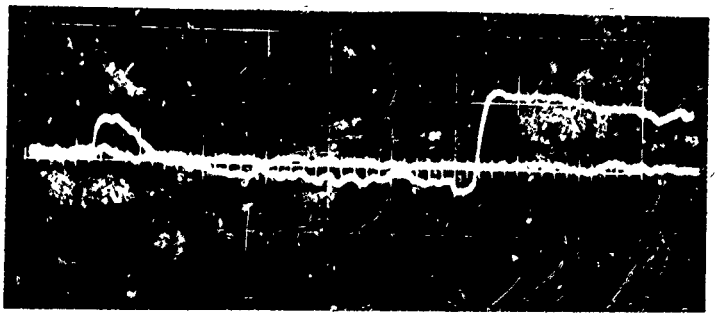

d) P_1=30mmHg

Fig. 5. Absorption Traces of NH_3 behind Detonations with N_2H_4. λ=2500 Å

Even though the curvature of the detonation front involves a rise time of the initial absorption signal of about 5 μsec, the signal's whole length of about 20 μsec is not accounted for by the absorption of hydrazine. Hence it is ascribed to ammonia.

Following the initial absorption peak, the trace drops off, explainable partly by volume expansion, partly by a decrease in temperature which involves lowering of the extinction coefficient of NH_3, and partly by the thermal decomposition of NH_3.

After a period of time, which covers 263 to 310 μsec from the passage of the detonation front on, the reflected wave compresses and heats up the reaction products such that renewed absorption is manifested.

The following table summarizes some of the observed quantities from records in fig. 5. P_1 is the initial pressure of hydrazine at 340 °K, ρ_1 the gas density in front of the detonation, t_r is the time elapsed between passage of detonation and reflected wave through the recording light beam, I_o is the calculated value of the light intensity without any absorption in the gaseous phase. I_o/I_i is the maximum absorption right behind the detonation front, attributed to an intermediate stage of the reaction, and I_o/I_5 is the maximum absorption behind the reflected shock wave.

Table II

	P_1 [mm Hg]	t_r [μsec]	I_o [V]	$\rho_1 \cdot 10^6 \left[\frac{\text{mole}}{\text{cm}^3}\right]$	log I_o/I_i	log I_o/I_5	α	β
a)	90	262	0.49	4.23	0.67	0.36	1.6	0.53
b)	60	290	0.40	2.8[illegible]	0.44	0.40	1.6	0.92
c)	40	308	0.47	1.89	0.33	0.44	1.7	1.3
d)	30	305	0.56	1.42	0.30	0.48	2.1	1.6

Since the conditions (temperature, density) behind the detonation front are basically unknown no statements about the NH_3 concentrations can be made at this point. Moreover, the curvature of the shock front makes it impossible to measure the initial absorption of decomposing NH_3 behind the detonation front (cf. p. 43).

IV. DISCUSSION

Speedy detonations are followed by nonsteady rarefaction waves. The distribution of density and local velocity has been dealt with theoretically and experimentally (ref. 39, 40). In this case, however, the starting conditions for the development of these detonations are rather complicated because they are initiated by H_2/O_2 detonations after rupturing of a diaphragm.

In addition to this, the oscilloscope records of fig. 5 indicate that ample quantities of NH_3 are present even at the point where the wake of the detonation interacts with the reflected shock. Since the measured detonation velocity corresponds closely to a theoretical value, which was calculated on the assumption that no NH_3 is left in the CHAPMAN-JOUGUET state, one should conclude that the reaction period is not at an end even 260 - 300 µsec after the detonation front has passed the recording light beam. Under ideal conditions rarefaction waves should not pass beyond the CHAPMAN-JOUGUET region because of the limiting condition for the local flow velocity M = 1.

On the other hand , these detonations are not really stable, even though the detonation velocity is reproducible and does not show any dependence upon the composition of the initiator gas.

The series of oscillograms in fig. 5 together with the evaluated data in tab. II illustrate a pronounced pressure dependence of the absorption as well as of the time interval between recording detonation front and reflected wave. This should not be expected for stable hydrazine detonations, because the CHAPMAN-JOUGUET temperature of 2000 °K is too low to induce any appreciable dissociation of reaction products. Also the density profile in the expansion fan should be independent of pressure in such a case (ref. 39). In these experiments, the reflected waves take more and more time before they cross the UV beam and relatively more and more ammonia appears behind both the detonation front and the reflected shock the lower the starting pressure P_1 is. The variation in the stoichiometry of the reaction is demonstrated by the dimensionless parameters α and β (table II).

α represents the logarithm of the measured initial absorption $\log I_o/I_i = \varepsilon(T_i) \cdot x \cdot \varrho_i(NH_3)$, divided by the initial density of hydrazine ϱ_1. $\varepsilon(T_i)$ is the extinction coefficient of NH_3 at 2500 Å and $\varrho_i(NH_3)$ the partial density of ammonia. Measurements of the temperature dependence of NH_3 are being made ($\varepsilon(T)$ has been determined only up to wavelengths of 2400 Å so far, ref. 7). In any case, without assuming a definite stoichiometry of the hydrazine decomposition neither the temperature course nor the profile of total density across the reaction zone can be calculated. But for stable detonations the ratio of densities in the initial gas and at the observable intermediate reaction stage could be expected to be the same at all pressures. This is not born out by the present evaluation as shown by the change in α, which indicates an increase in the relative ammonia production with decreasing pressure.

β is defined as the ratio $\frac{\log I_o/I_5}{\log I_o/I_i} = \frac{\varepsilon(T_5) \cdot \rho_5(NH_3)}{\varepsilon(T_i) \cdot \rho_i(NH_3)}$.

This quantity is a criterion for the amount of NH_3 which has decomposed in the time interval between recording of the detonation front and the reflected shock (subscript 5 denotes parameters behind the reflected shock). Despite the fact that this time interval increases, more and more ammonia survives in the wake of the detonation with decreasing detonation pressure. β grows from 0.53 at P_1 = 90 mm Hg to 1.6 at P_1 = 30 mm Hg. This might be explained in terms of a temperature decrease due to the interaction with expansion waves from both the walls and the initiation end of the tube.

On the assumption that hydrazine decomposes within a fraction of a μsec according to $N_2H_4 \longrightarrow NH_3 + 1/2\ N_2 + 1/2\ H_2$, followed by the slow pyrolysis of NH_3, and that the effects of expansion waves are negligible within the observation time of about 300 μsec, the course of temperature, density ratio and local Mach number have been calculated (fig. 6). As before, indices F, i, CJ and 5 denote conditions of the initial gas, at the shock front, at the point where hydrazine has decomposed but where all NH_3 is still present (see above), in the CHAPMAN-JOUGUET state and behind the reflected shock, respectively, It is interesting to note, that the temperature in the reaction zone exceeds the one in the CHAPMAN-JOUGUET state.

On the basis of this model, one may relate the measured absorption values of NH_3 behind the detonation, to reproduce the profiles of partial density of NH_3 and temperature. Rough estimates indicate a surprising consistency of temperature,

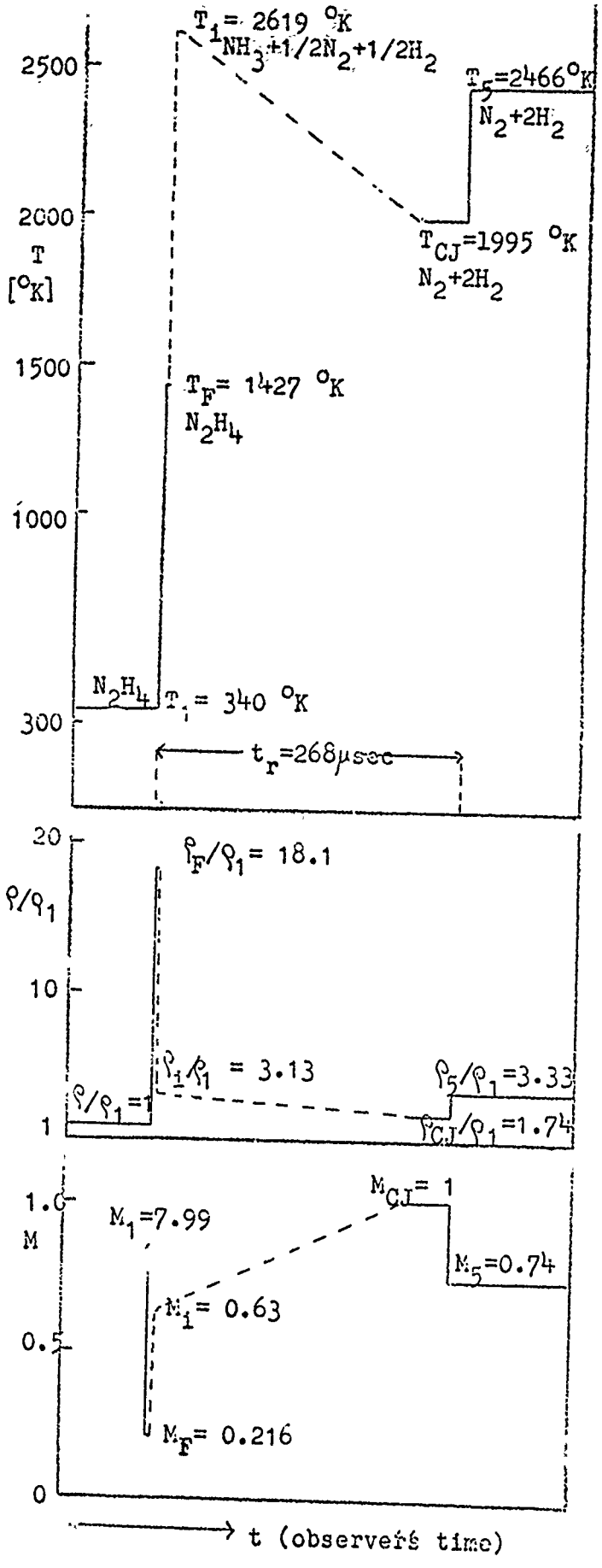

Fig. 6

Detonation Conditions (with D = 2.488 mm/μsec) governed by the reaction $N_2H_4 \longrightarrow NH_3+1/2H_2+1/2N_2 \longrightarrow N_2 + 2\,H_2$

P_1 = 90 mm Hg

P_F = 9.0 atm.

P_i = 2.85 atm.

P_{CJ} = 1.21 atm.

P_5 = 2.86 atm.

density and kinetic data of the NH_3 pyrolysis, known from previous measurements (ref.7). The calculated value for the speed of the reflected shock, travelling through the detonation wake in the CHAPMAN-JOUGUET state is u_5 = 1.15 mm/μsec. (Calculation of the conditions behind the reflected shock in fig. 6 is based on the assumption that the reaction has come to an end before the reflected shock appears, such that any further reaction behind the reflected shock could be ignored. The dissociation $H_2 \longrightarrow 2H$ was accounted for. Fig. 6 applies only to an idealized stationary detonation). Further approximate calculations show that the speed of the reflected shock is scarcely influenced by amounts of unreacted ammonia in the wake or by expansion waves from the initiation end (estimated according to ref. 39). u_5 varies between 1.15 and 1.07 mm/μsec. This result in computed values for the time interval t_r between 268 and 275 μsec. The experimental values for P_1 = 90 mm Hg range from 263 to 270 μsec. This consistency is most likely fortuitous and has to be examined more stringently. At lower initial pressures than P_1 = 90 mm Hg, the observed values for t_r are as high as 310 μsec. This suggests that other effects are operative besides phenomena associated with stationary one-dimensional detonations.

Within these cursory studies an interesting type of detonation has been considered. The gradual variation of the quantities t_r, α and β with pressure suggests that all of these detonations under the conditions used are inherently unstable despite reasonable values for the instantaneous detonation velocity. Nevertheless, one may expect, that under more favourable initial conditions they become stable.

C. Results from Shock-Wave Studies of the Decomposition of N_2O

I. INTRODUCTION

To interpret the observations of hydrazine-nitrous oxide detonations reported in section A, a more intimate knowledge of the thermal decomposition of both hydrazine and nitrous oxide is required. For this purpose, some results of shock-tube experiments with N_2O might ultimately provide supplementary information, apart from the fact that they are interesting for themselves.

The kinetics of the N_2O decomposition has been the subject of a number of investigations. The results of studies at temperatures below 1100 ^oK have been summarized by JOHNSTON (ref. 17). Some work has been devoted to details of the initial activation process in the unimolecular reaction (ref. 18 - 2o) and to the individual rates of secondary steps (ref. 21 - 23). These have indicated a number of uncontrolled complications, which preclude any extrapolation from these data to higher temperatures. Investigations at high temperatures have introduced some interesting technical innovations but have yielded somewhat divergent results (ref. 24 - 26). The shock-tube experiments in process are expected to provide some reliable information. Because the N_2O decomposition is exothermic, reflected shock waves had to be used (ref. 7).

II. EXPERIMENTAL

The same shock tube including the photoelectric recording technique used for the investigation of hydrazine and ammonia and described in ref. 6 and 7 serves for the reexamination of

the N_2O decomposition. As outlined before, shock parameters were calculated by iteration from the velocity of the incident shock, the attenuation of which was known.

In preparing the test gas, the flow velocities of Ar and N_2O (controlled by means of capillary flow meters) were set in the desired proportion. The gases were mixed before they entered the evacuated shock tube. Nitrous oxide (cf. p.7) and tank argon for welding (ref. 7, p.41) were used without further purification.

Two series of measurements at two different pressures can be reported now, both covering a range of Mach numbers from 2.55 to 2.80, involving reflected shock temperatures between 1550 and 1850 ^{o}K at reaction pressures of about 2 and 6.6 atm.

Records of N_2O reactions at temperatures higher than 1850 ^{o}K have been excluded in the present report because of uncertainties in the reaction conditions. Gas mixtures investigated so far contained 0.9 and 1.9 mole% N_2O in Ar. Such high concentrations involve considerable thermal effects during the time in which they react behind reflected shock waves. A simple estimate of these reaction conditions, based upon interpolation between two cases of stationary reactive flow that are amenable to exact computation, has been outlined in ref. 7. This method, however, requires knowledge of the final product composition (N_2, O_2 and NO) and of the enthalpy of the reaction. Previous work (ref. 23) did not provide this information. Thus, the present evaluation had to be restricted to the initial stages

of the reaction, where thermal effects are negligible, and to decompositions that proceeded slowly enough so as not to accelerate the reflected shock. Thus the initial temperature of the reaction corresponded closely to the temperature of the reflected shock calculated by ignoring any reaction whatsoever. At Mach numbers higher than 2.95, reflected shock speeds were measured which revealed a definite acceleration of the reflected wave. Thus, besides records of the reaction rate, another criterion was available to determine the point up to which the initial reaction conditions could be given by the simple shock-wave theory. Possibilities for measuring the exact proportion of NO among the reaction products will be outlined below (p. 43).

As with hydrazine and ammonia, the density profile of N_2O was followed on the basis of its absorption of ultraviolet light at wave lengths between 2250 and 2400 Å. The station for photoelectric recording was situated 10 cm upstream from the reflecting plate. The effective beam width of the UV light amounted to about 0.7 mm. With an average reflected shock speed of 0.48 mm/μsec, this resulted in a maximum time resolution of 1.5 μsec. Accordingly, the electrical time constant of the recording unit was chosen to be 1 μsec.

III. RESULTS

a) Light Absorption of N_2O

It was extremely conducive to the success of these investigations that nitrous oxide exhibits an unexpectedly high increase of light absorption with an increase in temperature. Literature

data of extinction values in the wave-length interval from 2100 Å to 2600 Å (continuous absorption, ref. 27) at room temperature did not furnish much hope that photoelectric techniques might be useful in this instance. Fig. 7a,b and 8a, b show oscilloscope records of the absorption traces. The base line results from the photocurrent of the full intensity of the incident light (applied after each experiment). The first step of the absorption trace, clearly discernable only for wave lengths $\lambda < 2300$ Å occured as the incident shock front passed by. As the reflected wave crossed the recording light beam, strong absorption appeared with subsequent decomposition of N_2O at a rate which depends upon the shock strength.

Despite the long rise time of the absorption signals (occasionally up to 10 µsec), indicating curvature and tilt of the shock fronts, the decomposition of N_2O proceeded so slowly at temperatures below 1800 °K that reliable evaluation of the initial absorption was possible. Fig. 9 shows the derived extinction coefficients in dependence upon computed temperatures. For the monochromator the following slit widths were used at the various wave lengths involving the dispersion values given below:

λ [Å]	2200	2250	2300	2400	2500	2600
s [mm]	0.5	0.3	0.2	0.18	0.16	0.12
$d\lambda/ds$ [Å/mm]	22	24	27	31	37	42

The increasing dispersion of the monochromator and the widening of the slit (in order to make up for the decrease in both the sensivity of the photomultiplier and the intensity of the light source) largely compensate each other, such that the spectral band

Records of Absorption behind Shock Waves with N_2O

Fig. 7

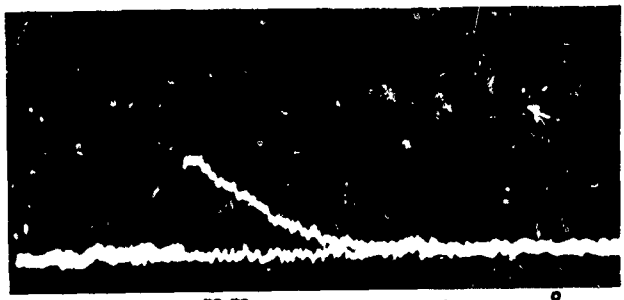

a) $U_1 = 0{,}874 \frac{mm}{\mu sec}$ 1,95% N_2O $\lambda = 2300 Å$

$\frac{U_5}{U_1} = 0{,}531$ $\varrho_5 = 9{,}6 \cdot 10^{-7} \frac{mole}{cm^3}$ $I_o = 1{,}9V$

$T_5 = 1755°K$ $k_1 = 2{,}6 \cdot 10^3 sec^{-1}$ $\varepsilon_5 X = 22 \cdot 10^5 \frac{cm^3}{mole}$

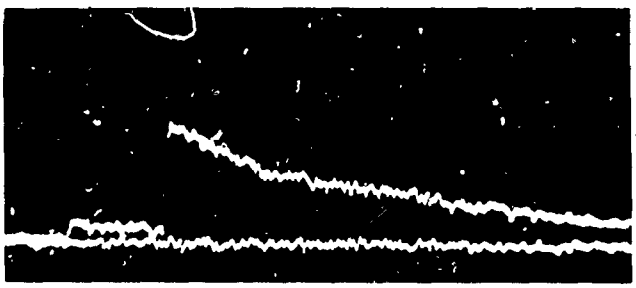

b) $U_1 = 0{,}876 \frac{mm}{\mu sec}$ 1,92% N_2O $\lambda = 2250 Å$

$\frac{U_5}{U_1} = 0{,}553$ $\varrho_5 = 8{,}8 \cdot 10^{-7} \frac{mole}{cm^3}$ $I_o = 2{,}0 V$

$T_5 = 1758°K$ $\varepsilon_5 X = 3{,}0 \cdot 10^5 \frac{cm^3}{mole}$

sweep 200 μ sec/cm; 0,5 V/cm

Fig. 8

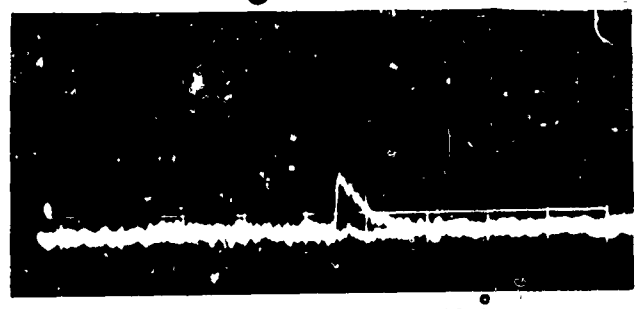

a) $U_1 = 0{,}958$ 1,55% N_2O $\lambda = 2400 Å$

$\frac{U_5}{U_1} = 0{,}532$ $\varrho_5 = 5{,}2 \cdot 10^{-7} \frac{mole}{cm^3}$ $I_o = 1{,}7V$

$T_5 \approx 2080°K$ $k_1 = 1{,}5 \cdot 10^4 sec^{-1}$

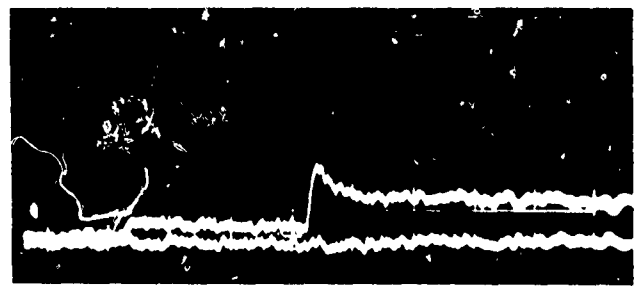

b) $U_1 = 0{,}955$ 1,54% N_2O $\lambda = 2250 Å$

$\frac{U_5}{U_1} = 0{,}553$ $\varrho_5 = 5{,}2 \cdot 10^{-7} \frac{mole}{cm^3}$ $I_o = 1{,}6 V$

$T_5 \approx 2070°K$

sweep 100 μ sec/cm; 0,5 V/cm

Records of Emission during N_2O Pyrolysis

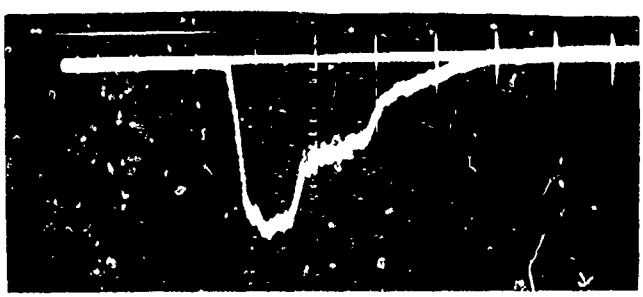

c) half-width of the first stage 200 μ sec

1,8 % N_2O

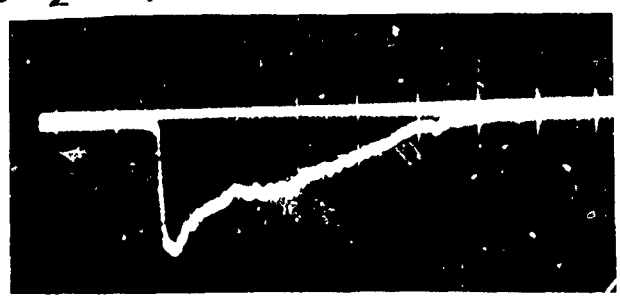

c) half-width of the first stage 60 μ sec

1,8 % N_2O

sweep 200 μ sec / cm; 0,2 V/cm

width is of the same magnitude throughout the wave-length interval.

In general, data from incident and reflected shocks match satisfactorily. No systematic dependence upon pressure or concentration could be detected.

In fig.10 the averaged extinction coefficients have been replotted versus wave length in order to illustrate the broadening of the whole absorption band with increasing temperature.

b) Light Absorption of NO

At wavelengths around 2250 Å, the absorption trace does not fall back to the zero line, as illustrated particularly by fig. 8 b. Since some bands of the γ-system of NO are situated in this region (0,0 and 1,1 transition) the persisting absorption might be caused by the reaction product NO (the fall-off in fig. 7b is probably caused by cooling and expansion waves, the effect of which is shown because of the slow sweep speed of 200 μsec/cm). Data about the kinetics of the NO decomposition behind shock waves (ref. 28) suggest that the rate determining reaction $2\ NO \rightarrow N_2 + O_2$, with $k = 4.8 \cdot 10^{23} \cdot T^{-5/2} \cdot \exp(-85\,500/RT)$ cm^3/mole·sec would involve a half-life of NO not shorter than 0.1 sec below 2000 °K, as soon as N_2O has disappeared. Hence, the reaction product can be considered as practically stable behind these reflected shock waves, even though the equilibrium proportion of NO at 2000 °K is not more than 1 mole% of the sum of N_2 and O_2. The concentration of NO appearing at the end of the N_2O decomposition can be determined from the remaining absorption at this point if the extinction coefficients of NO are known. This will also provide knowledge of

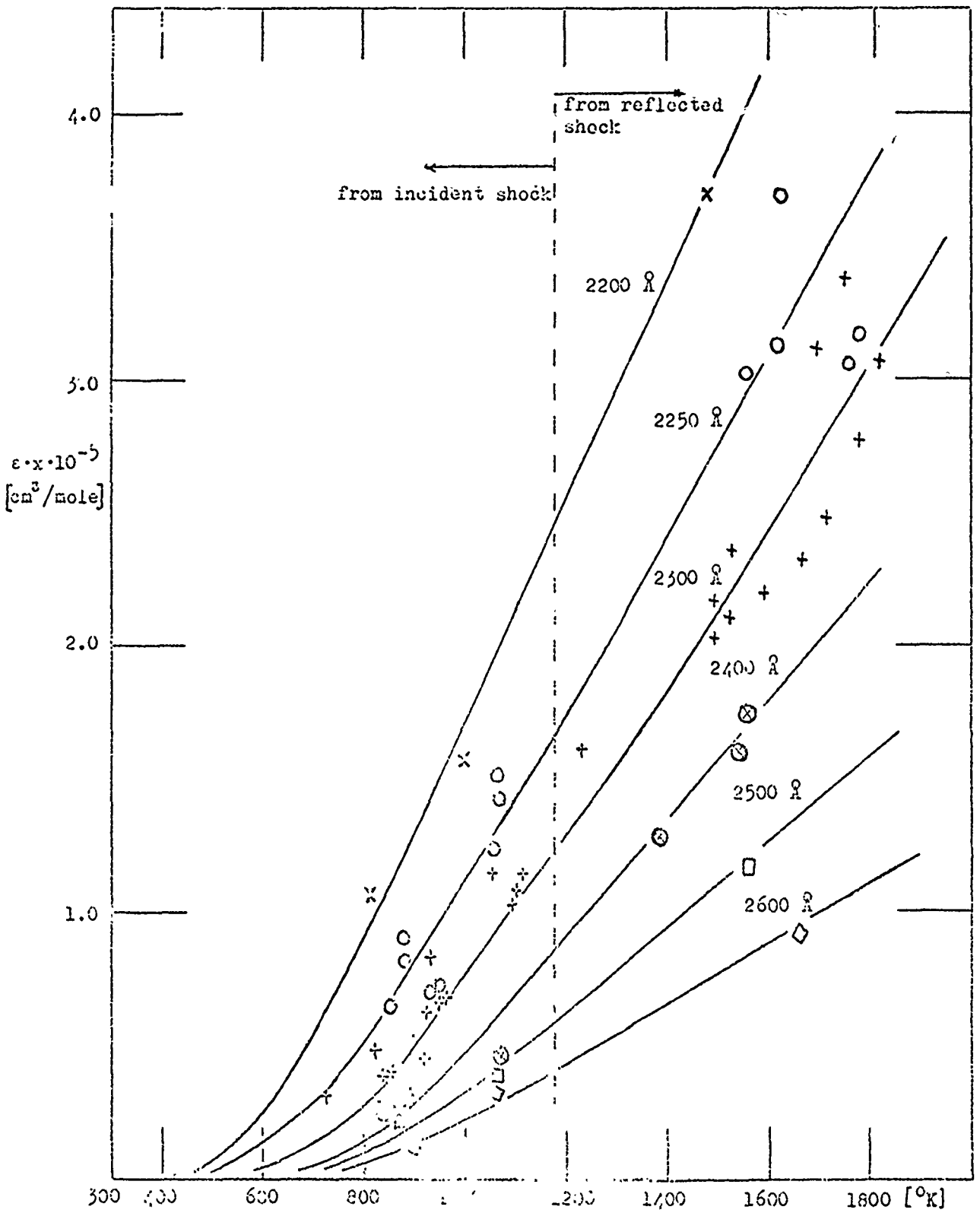

Fig. 9. Effective extinction coefficients of Nitrous Oxide vs. Temperature

× λ = 2200 Å + λ = 2300 Å □ λ = 2500 Å

○ λ = 2250 Å ⊘ λ = 2400 Å ◇ λ = 2600 Å

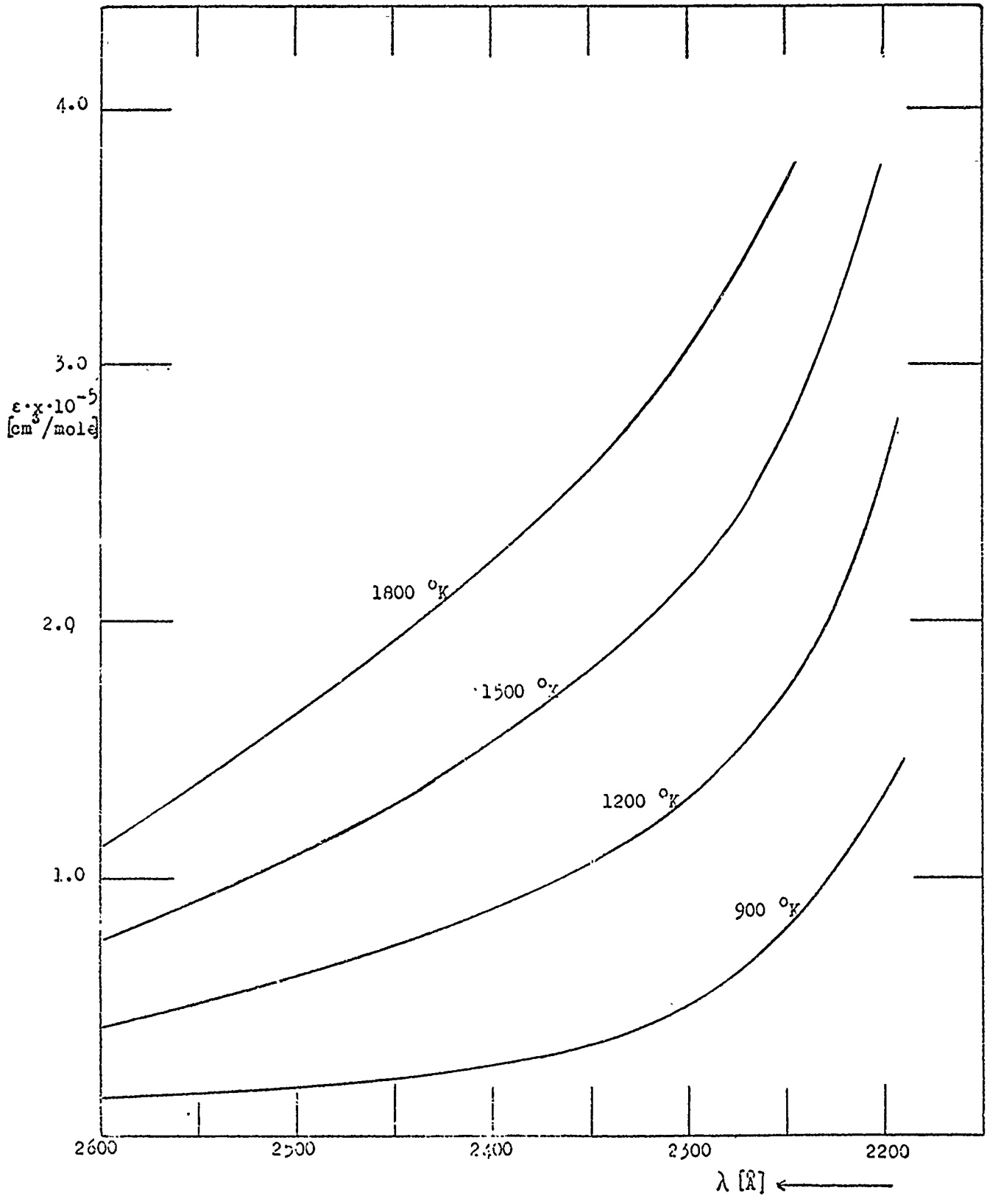

Fig. 10. Effective Extinction Coefficients of Nitrous Oxide vs. Wave Length

the stoichiometry and of the enthalpy of the N_2O decomposition. Then the exact reaction conditions are accessible to computations, and investigations can be extended to appreciably higher temperatures. Experiments for the quantitative determination of the light absorption by nitrous oxide at high temperatures are in progress.

c) Initial Decomposition Rates of N_2O

Since the over-all heat of the N_2O reaction is still unknown under these conditions, it would be premature to evaluate the whole of the absorption trace from kinetic aspects. The initial rate of decomposition, however, will not be affected by thermal self-acceleration. The major steps in the thermal decomposition of this quasi-unimolecular reaction are generally believed to be (ref. 21, 24, hot atoms as suggested in ref. 20 will be insignificant with an excess of inert gas):

(1) $N_2O \longrightarrow N_2 + O$

(2) $O + N_2O \longrightarrow N_2 + O_2$

(2') $O + N_2O \longrightarrow 2\ NO$

(3) $NO + N_2O \longrightarrow N_2 + NO_2$ $\quad k_3 = 2.5 \cdot 10^{14} \exp(-50\,000/RT)\ cm^3/mole \cdot sec$ (ref. 29)

(4) $NO_2 + N_2O \longrightarrow N_2 + O_2 + NO$

(5) $M + O + NO \longrightarrow NO_2 + M$ $\quad k_5 = (2 \text{ to } 4) \cdot 10^{16}\ cm^6/mole^2 \cdot sec$ (ref. 26)

(5') $O + NO \rightarrow NO_2^* \rightarrow NO_2 + h\nu$

(6) $M + O + O \longrightarrow O_2 + M$ $\quad k_6 = 2 \cdot 10^{17} \cdot T^{-1}\ cm^6/mole^2 \cdot sec$ (ref. 30, 31)

No other rate constants than k_3, k_5 and k_6 are known with any certainty. Some further thermal decomposition steps of NO_2 (ref. 32)

are irrelevant for the consideration of the initial reaction rate of N_2O. The radiative recombination of NO and O(5') forming NO_2 was estimated to account for only a small fraction (about 10^{-3}) of the termolecular reaction (ref. 21).

For the disappearance of N_2O, the following rate expression results:

$$- d[N_2O] /dt = k_1 [N_2O] + (k_2 + k_2')[N_2O][O] + k_3[N_2O][NO] + k_4[N_2O][NO_2]$$

In evaluating initial rates, it is sufficient to assume that [O], [NO] and $[NO_2]$, as well as additional terms which account for thermal self-acceleration, increase linearly with time:

$$- d \ln [N_2O]/ dt \approx k_1 + \alpha \cdot t$$

The oscilloscope records (such as fig. 7a and 7b) were smoothed and plotted in a concentration scale. By taking the difference $\Delta \ln[N_2O]$ per time Δt in the various reaction stages, one was able to extrapolate to the point t = 0, the beginning of the reaction, thus obtaining the first order rate constant k_1, which is assigned to the unimolecular decomposition of N_2O. Because of the slow rise time of the absorption signals, conditions at the start of the reaction were somewhat obscured in the records. Fig. 11, however, is a typical extrapolation plot for k_1, which illustrates that this procedure will not be compromised by too large an error. There is a monotonous increase of the formal first-order rate constant with time up to the point where the evaluation of the oscilloscope records becomes impossible because of too low absorption values.

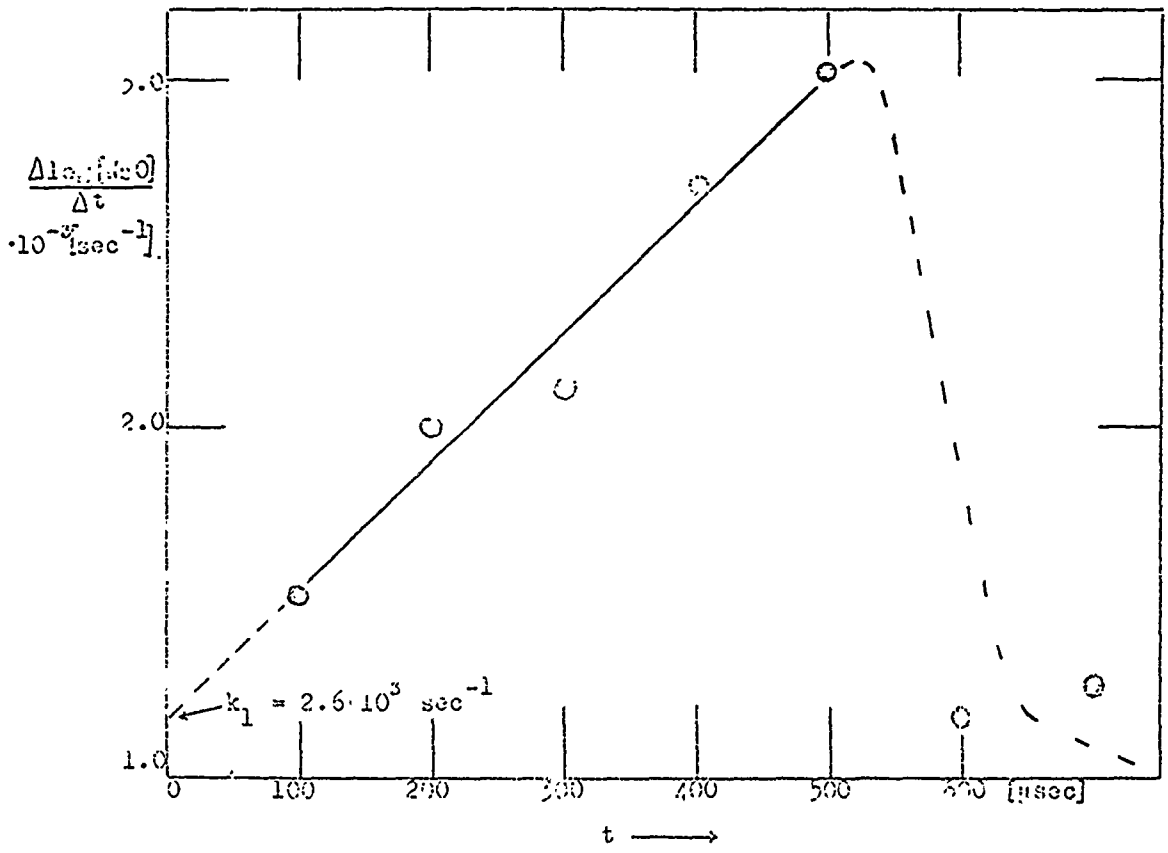

Fig. 11 Extrapolation Plot for Initial Rate, Corresponding to fig. 7a.

Fig. 12 is the Arrhenius plot of these initial rate constant derived in this way. Data from experiments at temperatures between 1530 and 1820 ^{o}K and at total gas densities of $0.45 \cdot 10^{-4}$ mole/cm^3 suggest a temperature dependence of $k_1 = 10^{10.8} \exp(-60\,000/RT)$ sec^{-1}. This compares favourably with the rate expression at lower temperatures $k_1 = 10^{10.72} \cdot \exp(-59\,400/RT)$ sec^{-1} at gas densities of $0.25 \cdot 10^{-4}$ mole/cm^3 (Ref. 17).

Some points from experiments at appreciably higher total gas densities are included in fig. 12. Because only initial rates are considered here, a comparison with the low pressure results is justified, despite the somewhat different partial densities of N_2O.

At the initial stages of the reactions, different total pressures will affect only the collisional activation of the unimolecular reaction step. Comparison of results from low and high pressure experiments disclose that the unimolecular decomposition of N_2O

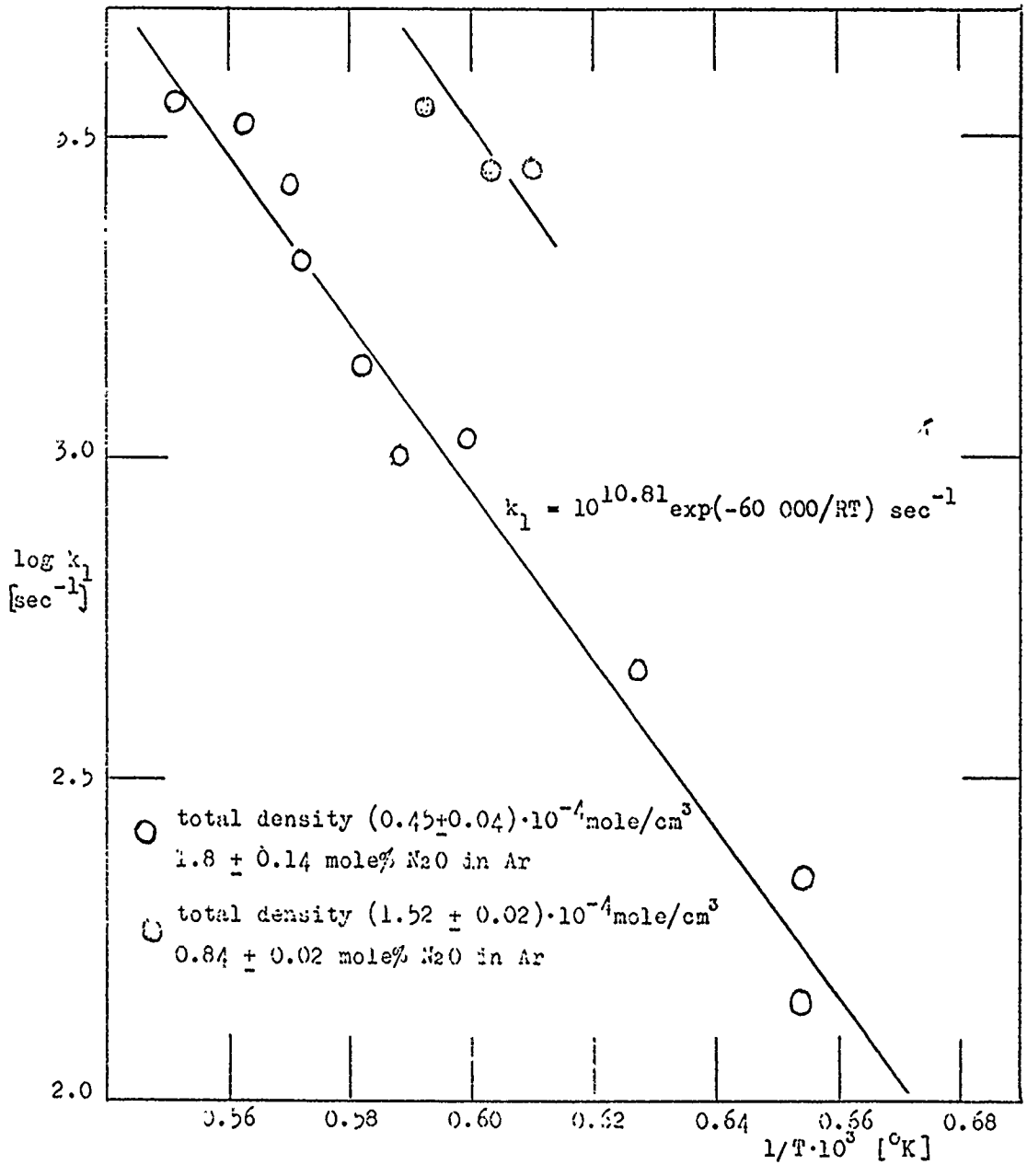

Fig. 12. Arrhenius Plot of the Initial First-Order Rate Constants in the Pyrolysis of N_2O.

is strictly regulated in this temperature range by bimolecular activation, viz. it is close to its low-pressure limit. The activation energy of 60 kcal/mole is still comparatively high as compared to the literature values which range down to 50 kcal/mole. This is contradictory to the predictions of unimolecular rate theory, which requires a fall-off of the activation energy as the low-pressure limit is approached (ref. 33). Implications of the dissociation of N_2O via forbidden triplet states, however, account for the exceptional behavior of this compound and have been discussed in the literature (ref. 18, 20).

Extension of these experiments to higher temperatures might further confirm these data. Assessment of the significance of various secondary reactions will be possible, when we know to what degree the heat of the reaction:

$N_2O \rightarrow N_2 + 1/2\ O_2 \quad \Delta H^0 = -19.46$ kcal/mole (300 °K) is compensated by the endothermic character of the competing decomposition mode

$N_2O \rightarrow 1/2\ N_2 + NO \quad \Delta H^0 = +2.12$ kcal/mole (300 °K).

The effect of thermal self-acceleration might possibly even outweigh the catalytic acceleration of the reaction by intermediate products under the present experimental conditions.

d) Spectroscopic Observations in Emission

Other work has indicated a typical chemiluminescence assigned to reaction (5') of nitric oxide with oxygen atoms (ref. 21,34). The glow is reported to appear as a continuous spectrum extending

from about 4500 to 6500 Å. Several experiments were made to observe the magnitude of this chemiluminescence and its dependence upon time and temperature during the decomposition of N_2O behind reflected shock waves. Even though this phenomenon has been observed before during the decomposition of N_2O, it was not certain at all, whether it would also appear with an excess of Ar, because added gases were shown to reduce the glow intensity appreciably (ref. 21).

A 2 mm wide section of the window at the lower end of the shock tube was imaged onto a RCA 931 A photomultiplier, the light passing on its way through SCHOTT interference filters (type A1, $\lambda_{max.}$ = 5620 Å, max. transmission 64 %, spectral half-width 200 Å, and another one with $\lambda_{max.}$ = 4090 Å, max. transmission 51 %). With the 4090 Å filter, scarcely any vertical deflection of the oscilloscope trace was recorded. With the 5620 Å filter, however, oscillograms of the kind reproduced in fig. 7c and 8c were obtained. The shock speeds, concentrations and partial densities of N_2O in fig.7c and 8c correspond closely to the values given in the legends of fig. 7a, b and 8a, b, resp. The emission signals are composed of two parts: a larger stage which commences with the arrival of the reflected shock and the half-period of which (200 and 60 μsec, resp.) coincides approximately with the half-lives of N_2O (220 and 40 μsec, resp.); moreover, there is a more persisting but lower luminescence which fades uniformly some 500 μsec after the passage of the reflected shock, probably explainable by cooling effects. The rise time of the former signal is strongly dependent on temperature. At 1760 °K (fig. 7c), it takes some 100 μsec to attain its full

height; at 2080 °K (fig. 8c), the rise time amounts only to 20 μsec (time resolution in these experiments approximately 4 μsec). Wave length dependence and simultaneity of this glow with the reaction are strong evidence for its being caused by radiative recombination of $NO + O \rightarrow NO_2^* \rightarrow NO_2 + h\nu$. Consequently, the emission intensity should be given by $I = k_5'(NO)(O)$, and it might be used to trace the change in the product of the concentrations [NO] and [O]. Under the present conditions, however, ample self-absorption seems to take place because the magnitudes of the emission signals are determined neither by the initial N_2O concentration nor by the reaction rate.

These cursory emission studies are relevant to this investigation of the N_2O decomposition in so far as the observed rise time to the peak intensities indicates that there is a slow build-up of the NO and O concentrations, followed by a decrease in either one of them or both. Hence there is a reaction period during which oxygen atoms probably exceed by far their equilibrium concentration.

Further work to investigate the pyrolysis of the oxidizer N_2O at high temperatures is in process.

D. The Thermal Decomposition of Hydrazine in Helium between 1400 °K and 1550 °K

I. PROBLEM

Investigations of the thermal decomposition of hydrazine behind shock waves, using Ar as a carrier gas, have indicated that the decomposition process is governed by a non-branching chain mechanism at partial densities of hydrazine of $20 \cdot 10^{-8}$ mole/cm^3 and in the temperature range from 1100 °K to 1400 °K (ref. 6 and 7).

Dependence of the half-lives upon temperature, concentration and pressure could satisfactorily be accounted for by a set of four reasonable rate constantes for the elementary reactions, the rate determining steps being the chain initiation:

$$N_2H_4 \longrightarrow 2\ NH_2 \qquad k_1 \approx 10^{14} \cdot e^{-60\ 000/RT}\ sec^{-1}$$

and a propagation reaction

$$NH_2 + N_2H_4 \longrightarrow NH_3 + N_2H_3 \qquad k_2 \approx 10^{13} \cdot e^{-12\ 000/RT}\ cm^3/mole \cdot sec$$

The temperature dependence of k_1 and k_2 given above allows extrapolation to a region between 1400 °K and 1500 °K. When $\rho_5 = 20 \cdot 10^{-8}$ mole/cm^3, one may calculate on the basis of an approximate relationship between half-life and these rate constants (ref. 7) that the apparent energy of activation obtained from half-life measurements and the activation energy of the unimolecular initiation step should not differ by more than 5 % in the temperature region above 1400 °K.

II. PROVISIONS FOR EXTENDING INVESTIGATIONS TO SHORTER REACTION TIMES

Previous measurements of hydrazine decomposition in Ar were confined for reaction times longer than ca. 15 μsec. Close to the shock front absorption signals were strongly distorted by schlieren-effects. The rise time of the signals upon shock passage amounted to as much as 5 μsec. To account for these effects, some correction procedure has already been given (ref. 6). But the corrections were sometimes of the magnitude of the measured quantity itself. Hence, no reliable kinetic information could be expected about hydrazine at temperatures higher than 1400 °K, where the half-life of the decomposition lies around 15 μsec.

The reliability of these measurements can not be improved unless

one is able to reduce the extent of the schlieren-effect and to account properly for the shock-front curvature. This can largely be achieved by using He as a carrier gas. For the same pressure gradients, the schlieren-effect in He is about eight times smaller than in Ar (refractive index of He $n = 1+0.36 \cdot 10^{-4}$, of Ar $n = 1+2.81 \cdot 10^{-4}$; cf. e.g. ref. 41).

In the absence of schlieren-effects, the rise time of the absorption signals upon shock passage depends upon shock speed and shock-front curvature (defined as the distance along the center line from the shock front to the plane formed by the intersection of the shock front and the shock-tube walls). Since the gases behind reflected shocks are quiescent, a faster rise time of the absorption signal also entails an improvement in time resolution. The rise time was determined to only a small extent by the effective width of the UV beam, which was 0.5 mm in these experiments (for its experimental determination see ref. 61). Hence, the attainable time resolution would have been 1 μsec with Ar as carrier gas and 0.35 μsec with He (the average reflected shock speeds were 470 m/sec and 1400 m/sec, resp.; the electrical time constant of the recording unit was chosen as ca. 0.5 μsec).

The oscilloscope recordes in Fig. 13 show passage of the incident and of the reflected shock in Ar (fig. 13a, M = 2.46, u_1=794 m/sec, 0.30 % N_2H_4, T_5 = 1500 °K, $\tau_{1/2}$= 4 μsec; for denottation and experimental details see ref. 6 and 7) and in He (fig. 13b, M = 2.46, u_1 = 2 453 m/sec, 0,49 % N_2H_4, T_5 = 1500 °K, $\tau_{1/2}$ = 5 μsec). A strong schlieren spike precedes the absorption increase across the incident shock in Ar. In the case of He, the schlieren effect

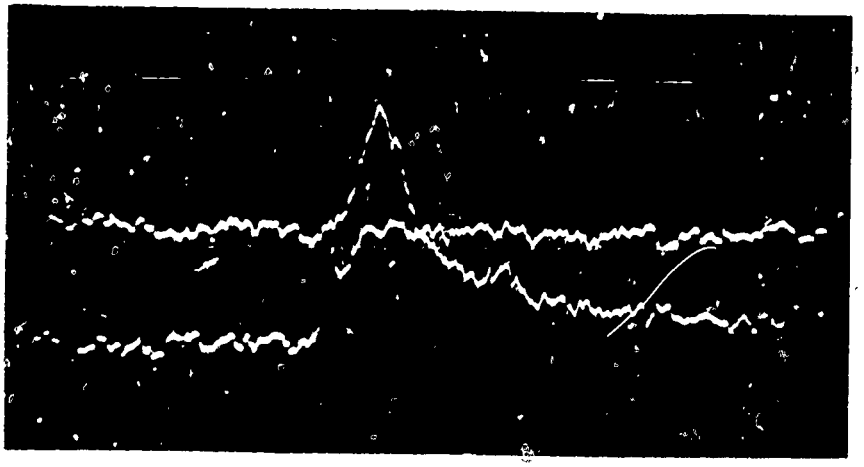

Fig.13a

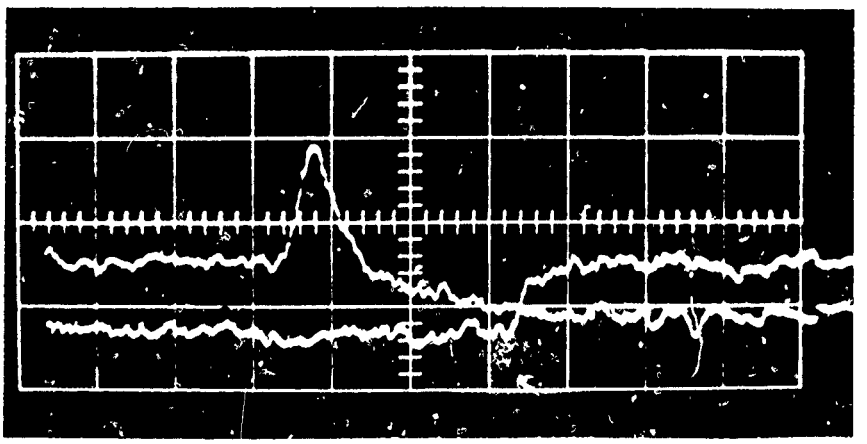

Fig.13b

is negligible as compared to the size of the absorption signal. In fig. 13a the rise time of absorption across the reflected shock front is 5 μsec, in fig. 13b it amounts only to 3 μsec. This slow rise time might be caused by the tilting of the shock surface relative to the UV beam or by shock-front curvature. Tilting would have manifested itself by random scattering of the experimental rise times. Since the experimental points show comparitively little fluctuation, shock curvature is more likely the proper explanation. The shock-front curvature, as defined above, would amount to 2.4 mm for Ar and 4.2 mm for He. As in LIN and FYFE'S findings for shock-front curvatures of incident shock waves, it does not seem to depend noticeably upon the shock speed (ref. 42 and 43).

Thus, the advantage of using He as a carrier gas is that the range of experiments can be extended to faster reaction rates. Absence of disturbing schlieren effects makes it possible to account for the displacement in time scale by the shock-front curvature when the reaction periods are comparable in length with the rise time of the absorption signal.

For the purpose of this evaluation, a simplified model of the reflected shock surface has been assumed (a more rigorous treatment of the curvature of the incident shock was given in ref. 43). Cooling which results from the formation of an eventually turbulent boundary layer in the wake of the incident shock before it interacted with the reflected wave, as well as bifurcation patterns and weak schlieren effects were ignored (cf. ref. 7). This was justified in the case of He. The bulging back of the reflected shock surface was approximated by an isosceles triangle, its height being equated with the experimental shock curvature of 4.2 mm, viz. 3 μsec

in time scale (fig. 14). For the sake of simplicity, the concentration of hydrazine is assumed to decrease linearly with time from the start of the reaction to its half-period (viz. no induction period):

$$\rho / \rho_5 \approx 1 - \frac{0.5}{\tau_{1/2}} \quad t$$

(ρ = instantaneous value of the partial density of N_2H_4, ρ_5 = initial value behind reflected shock; reaction time t and half-life $\tau_{1/2}$ both in μsec).

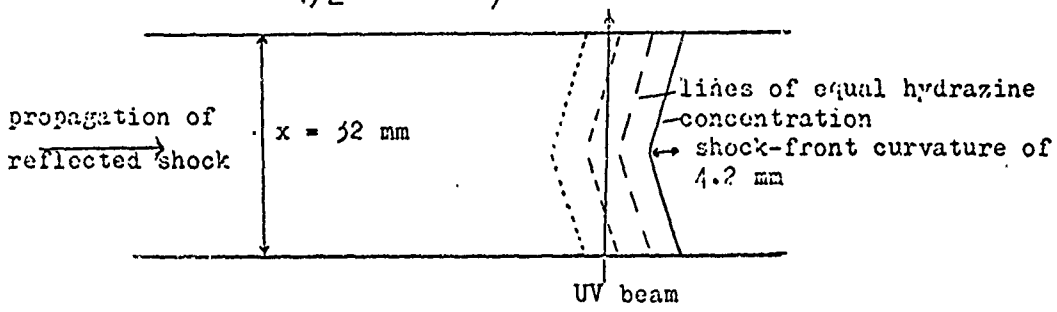

Fig. 14

The relative density of hydrazine along the path of the UV beam is then

$$\rho / \rho_5 = 1 - \frac{0.5}{\tau_{1/2}} \left[t + 3\left(1 - \frac{x}{16}\right) \right]$$

t is the time counted from the center of the shock front or in the oscilloscope records from the point of maximum absorption; x is the distance from the wall (because of symmetry, this is taken only to the meddle of the tube). Then the apparent degree of reaction is obtained by integration and normalization with half of the optical path length (16 mm):

$$\xi = 1 - \frac{1}{16} \int_0^{16} \rho / \rho_5 \, dx = \frac{0.5}{\tau_{1/2}} (t + 1.5)$$

It is obvious that the point of maximum absorption, where t = 0, does not any longer reflect the absorption of hydrazine

prior to the reaction, as it did in the studies made in the temperature range from 1100 °K to 1300 °K.

Then the induction period of the reaction was appreciably longer than the rise time of the absorption across the reflected shock. Now even at t = 0, the apparent degree of reaction appears to be ζ = 28.8 % for $\tau_{1/2}$ = 2.6 μsec and ζ = 7.5 % for $\tau_{1/2}$ = 10 μsec. The initial absorption behind the reflected shock cannot any longer serve as the basis for kinetic evaluation of the oscillograms. Instead of this, the exact concentration of hydrazine was derived from the step in the absorption trace, where the incident shock passed by, utilizing the known shock parameters for incident and reflected waves. The theoretical absorption behind the reflected wave prior to reaction could be computed then by extrapolating the curve for the temperature dependence of extinction coefficients to values beyond 1350 °K (fig. 15).

In practically all experiments with He as carrier gas, the difference between theoretical and measured extinction at the absorption maximum was equal to the apparent degree of reaction ζ, evaluated by means of the above expression at t = 0. This shows that the simplified model of the shock surface was a good approximation for the reduction of the present data. The quantity used to characterize the decomposition rate of hydrazine was the half-life $\tau_{1/2}$. The apparent half-life $\tau_{1/2}'$ was the time interval between the absorption maximum (t = 0) and the point where the measured absorption amounted to the apparent degree of reaction ζ = 1/2. From the expression given above, one derives then the

relation between $\tau_{1/2}'$ and $\tau_{1/2}$:

$$\tau_{1/2} \approx \tau_{1/2}' + 1.5\ \mu\text{sec}.$$

Hence, the displacement caused by the shock-front curvature corresponds to approximately half of the time interval necessary for the absorption signal to rise to its maximum value. The absorption at the point where $\xi = 1/2$ was obtained by back-calculation from the measured absorption behind the incident shock, using the known shock parameters and the extrapolated curve of the temperature dependence of the extinction coefficients.

Contrary to conditions at temperatures below 1300 °K, the absorption of ammonia appearing as a decomposition product of hydrazine could not be disregarded in these experiments. Assuming the stoichiometry of the reaction to be $N_2H_4 \longrightarrow NH_3 + 1/2 N_2 + 1/2\ H_2$ and using the known extinction coefficients of NH_3 (ref. 7, 15), it was found that, as half of the hydrazine had decomposed, the extinction of NH_3 amounted to approximately 10 % of the extinction of hydrazine. This was accounted for in the present evaluation.

Parameters of the incident and reflected shock waves were calculated as outlined in ref. 7. for He and Ar containing 0.2, 0.3 and 0.5 % N_2H_4. The acceleration of the reflected shock wave by the heat evolved during the reaction, was accounted for by assuming the case of stationary reactive flow, this having been shown to be adequate if the reaction goes to completion within less than 50 μsec (ref. 7). Moreover, the correction for non-isothermal character ΔT_e was added to the computed shock-front temperature. At M = 2.5, ΔT_e was 1.5°, 2.3° and 3.7 °C for carrier gases

containing 0.2 %, 0.3 % and 0.5 % N_2H_4, respectively (also for the case of stationary reactive flow, ΔT_e depends somewhat upon the flow velocity of the gas).

In evaluating the extinction coefficients behind the incident shock, the initial absorption of hydrazine was always considered.

III. RESULTS

A new shock tube having the same dimensions as the one described previously was used. The aluminum walls, however, had not been eloxized. Thus, it was necessary to check whether this in any way promoted the heterogeneous decomposition of hydrazine under the present conditions. The extinction coefficients measured behind the incident shock and reproduced in fig. 15 demonstrate that this was not the case. Nonetheless, in order to obtain this result, the shock tube had to be flushed with the reactant gases under the initial pressure of an experiment for the same lenght of time as in previous experiments. Under these circumstances, hydrazine seems to be adsorbed by untreated aluminum to approximately the same degree as by eloxized aluminum. The extinction coefficients measured in He up to temperatures of 830 ^{o}K confirm those obtained previously with Ar as a carrier gas.

The half-lives of the reactions in He and in Ar are the same (fig. 16). Thus, within the accuracy of these experiments, the decay of hydrazine above 3 atm. seems to be independent of the nature of the inert gas and of the total pressure. Due to the greater difficulties in the reduction of data at faster reaction rates, the scattering of the points is more pronounced than in

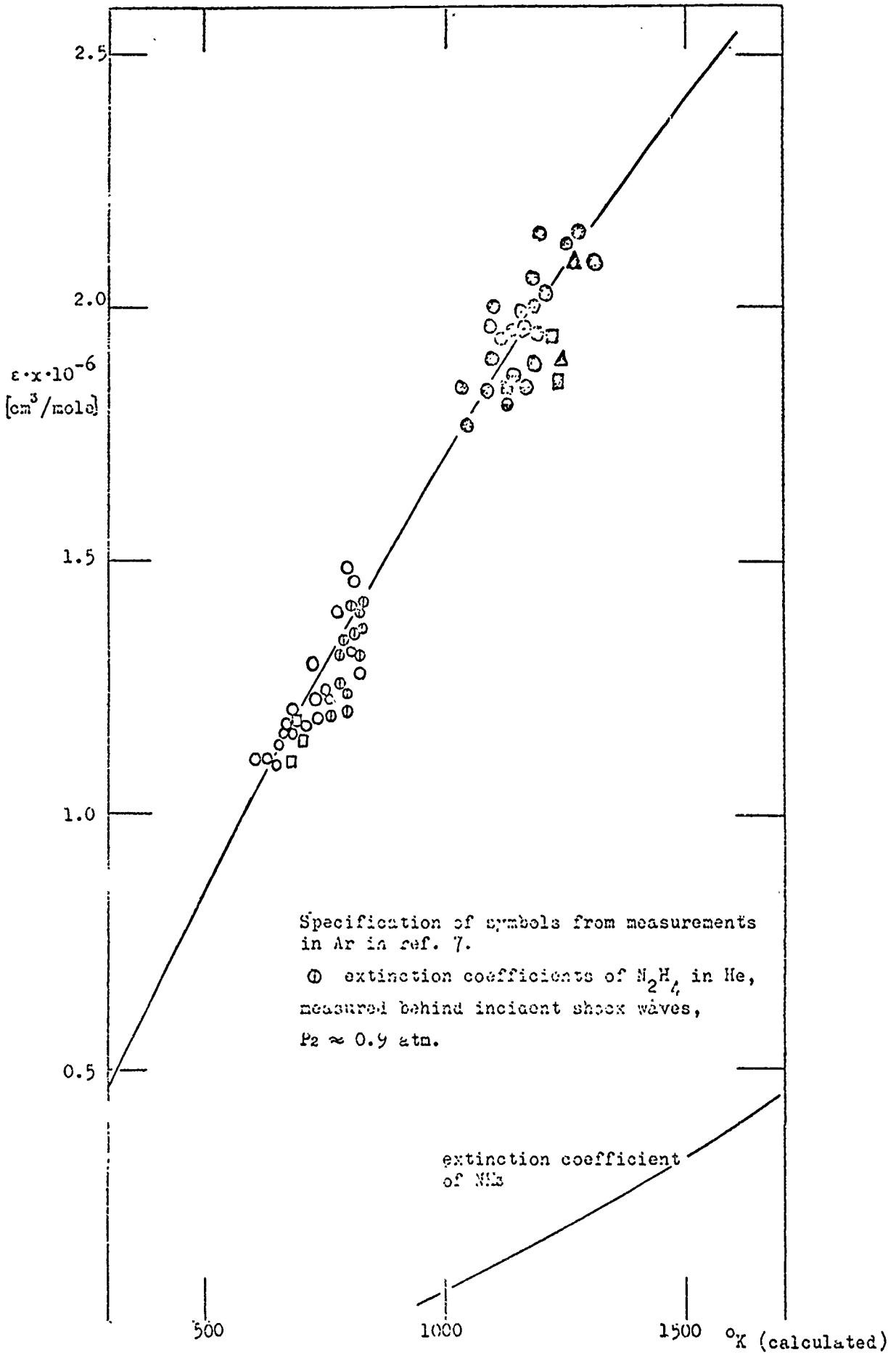

Fig. 1: Extinction coefficients of hydrazine in Ar and in He at λ = 2500 Å

the experiments reported previously. At temperatures above 1400 °K, no systematic relationship between half-lives and the partial density of hydrazine is detectable. The straight line in fig. 16 corresponds to an apparent energy of activation of 40 kcal/mole and was extended to temperatures of 1550 °K from points obtained previously in the interval from 1100 °K to 1400 °K. The half-lives of the decomposition rates which are supposedly governed to a larger extent by the unimolecular reaction exhibit an activation energy which does not seem to be different from that in the temperature range where the chain reaction has an appreciable share in the overall reaction rate.

IV. DISCUSSION

Despite the strong scattering, the points in fig. 16 clearly indicate that the apparent activation energy characterizing the decomposition of hydrazine above 1400 °K is not appreciably different from 40 kcal/mole. This result is surprising in that it has been shown that the chain reaction does not contribute much to the overall decomposition at these partial densities of hydrazine. Hence, this energy of activation will largely be ascribed to the unimolecular fission of the N-N bond. If E=60 kcal/mole is assumed to be the correct value for the critical energy of the N-N bond fission (ref. 44), then a decrement of about 20 kcal/mole would not agree with predictions of current theories dealing with unimolecular reactions.

SLATER'S theory (ref. 33) allows for a difference between measured activation energy and critical bond energy at low pressures

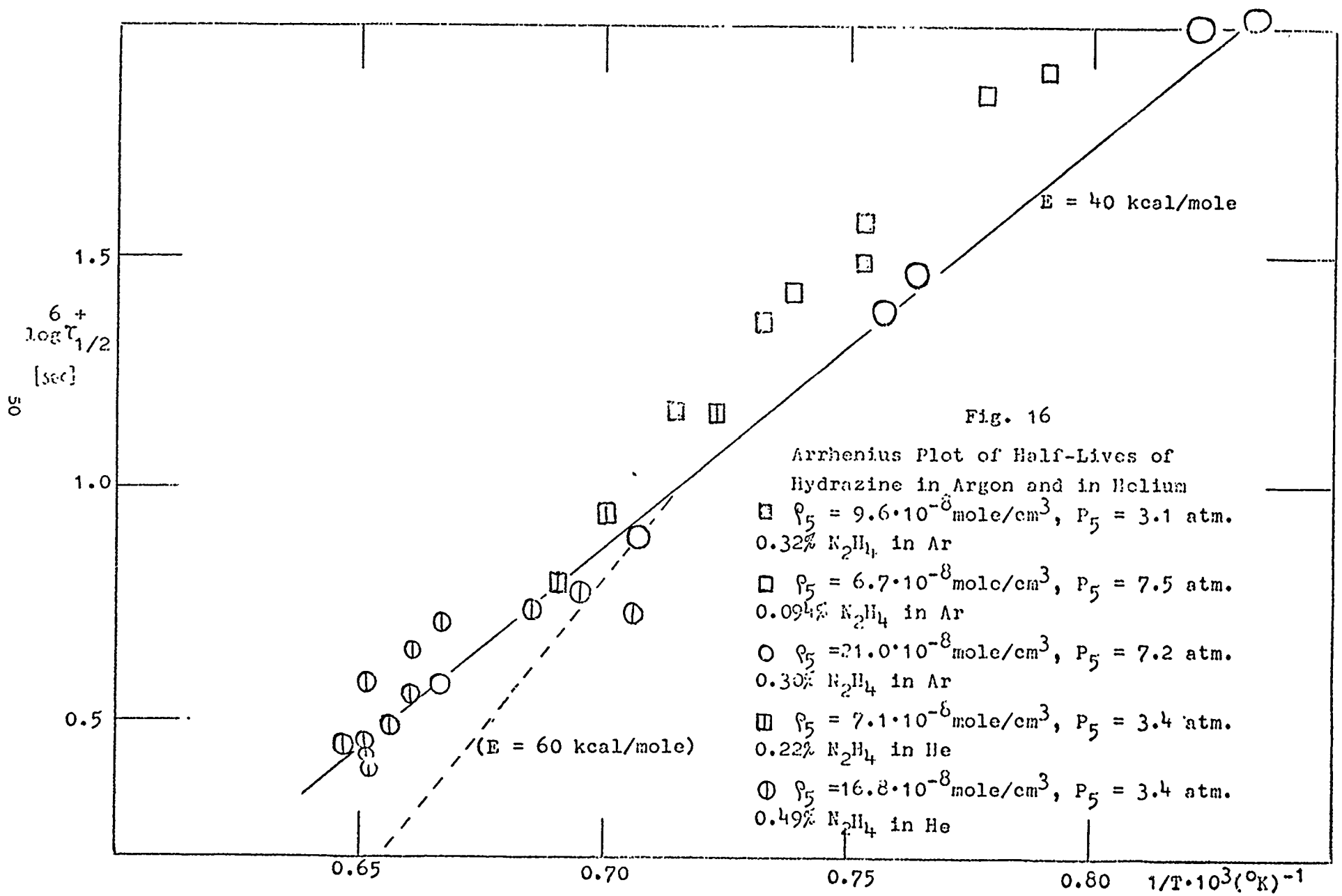

Fig. 16

Arrhenius Plot of Half-Lives of Hydrazine in Argon and in Helium

of as much as

$$\Delta E = \frac{n}{2} kT \cdot A_n(\Theta) \quad < 17 \text{ kcal/mole at } 1450\ ^{\circ}K,$$

where n denotes the number of effective modes of vibration (in hydrazine n = 12) and $A_n(\Theta)$ a factor which depends upon total pressure and varies between 0 (at the high pressure limit) and 1 (at the low pressure limit). Θ, the parameter proportional to pressure, is

$$\Theta = \frac{\omega}{\nu} \cdot f_n \cdot \left(\frac{E}{RT}\right)^{(n-1)/2}$$

where ω represents the collision frequency, ν a mean vibrational frequency and f_n a factor which, when n = 12, is about 7 (ref.33). For the conditions of the present experiments, one calculates with E = 60 kcal/mole and T = 1450 $^{\circ}K$ $\Theta = 10^5$, whence follows $A_n(\Theta) \approx 0.2$ (ref. 33, p. 186) and $\Delta E \approx 3.5$ kcal/mole. Thus, the apparent energy of activation should be fairly close to the high pressure value. In fact, the experimental result that the reaction is independent of pressure and that there are no inert gas effects would contradict the usual expectations for the behaviour of a unimolecular reaction at its low pressure limit. SLATER'S theory does not explain the discrepancy of 20 kcal/mole.

KASSEL'S model allows for a larger difference between apparent activation energy and critical energy at low pressures

$$\Delta E = n\ kT\ A_s(P) < 34 \text{ kcal/mole.}$$

But even this interpretation is suitable only if the reaction conditions are such that a definite decline of the first-order rate constant with pressure takes place.

It is curious that the bond dissociation energy given by SZWARC (ref. 44) was obtained as the activation energy of the bond fission reaction at pressures around 10 mm, which is lower by a factor of $4 \cdot 10^{-3}$ than the pressures prevailing in the present experiments. Thus, despite the higher temperature, these present shock tube investigations should have furnished an apparent energy of activation closer to the high-pressure value than SZWARC'S data.

The unexpected result that the activation energy does not change appreciably with temperature has to be examined more closely. To obtain more confidence in these shock-tube data, it is necessary to reduce the extent of deviations from ideal shock behaviour. This might be achieved by using a shock tube of a larger diameter.

E. Description of a New Shock Tube

I. INTRODUCTION

Studies of the pyrolysis of hydrazine, ammonia and nitrous oxide (cf. sections C and D) in a square shock tube, 3.2 cm on the inside, had revealed certain limitations in both the range of experimental possibilities and the reliability of the results. Due to the relatively thick boundary layer, appreciable deviations from ideal shock behavior appeared, such as attenuation of the shock speed, cooling effects to an extent which could not be ignored as well as a definite curvature in the shock surface. Even though the deviations from ideal behavior of the reflected shock, when interacting with an attenuated gas flow behind the

incident wave, and also the cooling effects could be accounted for semiquantitatively, the shock-front curvature involved a loss in time resolution and prevented the spectrophotometric registration of the concentration just behind the shock front at fast reaction rates. The optical path length of 3.2cm imposed a lower limit upon the concentrations of hydrazine, these being high enough then to produce material changes in the shock conditions due to the heat evolved and the increase in the number of particles during the reaction. It was necessary to apply corrections and the evaluation of the data was not without complications. Besides that, one cannot rule out that certain uncontrolled factors complicate the hydrodynamics of gas flowing through a pipe of square cross-section. In view of this, it seems obligatory to show that previous results were independent of the peculiarities of the technique.

So, a new shock tube was constructed which allows measurements for which these disturbing effects are greatly reduced. In particular, it was necessary to choose a larger cross-section for the tube.

II. CALCULATION OF THE SHOCK-TUBE DIMENSIONS

It appears that a round aluminum shock tube with 10 cm internal diameter provides a considerable improvement and comparatively clean-cut flow conditions. The dimensions of the high and low pressure parts were designed according to empirical rules concerning the path length for stabilization of a shock wave (ref. 45, 46) and according to the desired observation time of the reactions after shock reflection. For the most part, experiments with large excess of N_2H_4 are planned and the tube dimensions were calculated for this purpose. The prospective Mach number

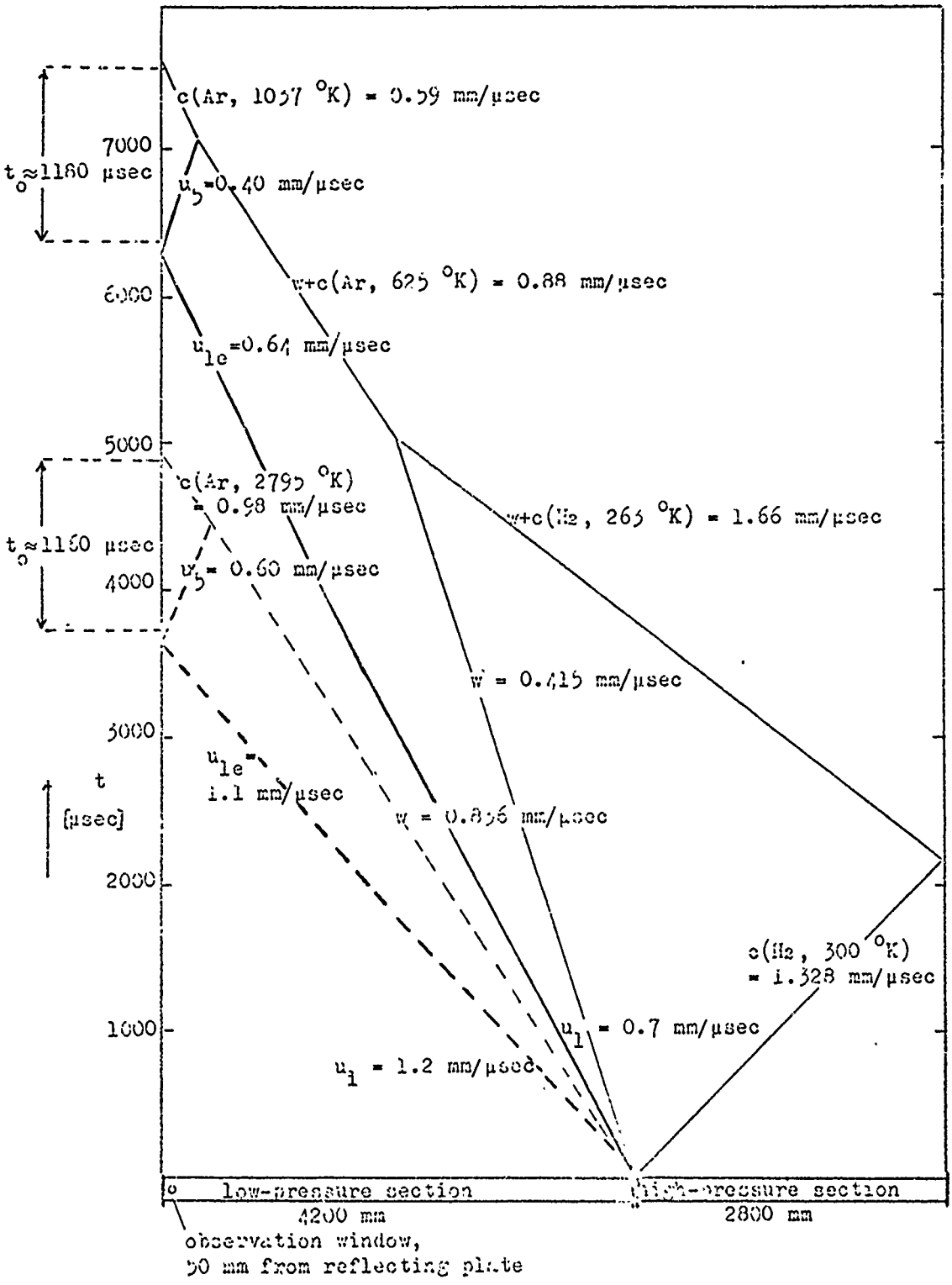

Fig. 17. Wave Diagram for M = 7.18 (solid lines) and M = 5.75 (dashed lines) in Ar.

range is 2.2. < M < 3.7, corresponding to initial shock speeds through Ar of 0.7 mm/μsec < u_1 < 1.2 mm/μsec. In the lower Mach number range, the observation time near the reflecting plate is limited by the arrival of the expansion waves from the high pressure part. In the higher range of Mach numbers it is the interaction of reflected shock and contact surface (since in general, the acoustic impedances of driver and test gas are not matched), which sets an end to well-defined reaction conditions near the observation window (fig. 17). Because of cooling effects, it is not meaningful to permit reaction periods much longer than about 1 msec behind reflected shock waves.

Fig. 17 shows the wave diagram for the described shock tube, consisting of a high-pressure section of 2.80 m length and a 4.20 m long low-pressure part. Conditions for initial Mach numbers M = 2.18 and M = 3.75 with initial speeds u_1 = 0.7 mm/μsec and 1.2 mm/μsec, resp., have been illustrated. A shock attenuation of 2 %/m has been assumed. Then for the above examples the effective Mach numbers (ref. 7) near the observation window are 2.0 and 3.44, resp., on the basis of which the reflected shock speeds were calculated. Because the exact computation of the velocity across the expansion fan (the corresponding flow conditions are not shown in fig. 17) is laborious, we took the speed of the first expansion signal from the point of reflection at the end of the driver section to the interaction with the contact surface as being uniformly the maximum speed, which is the sum of the sound velocity through expanded hydrogen c (H_2, 263 °K) and the flow velocity w. In the last effect, this gives a lower limit for the length of the useful observation period behind the

reflected shock. Beyond the contact surface, the first expansion signal travels at the sound speed of the Ar gas, which is heated by shock compression, superimposed to the flow velocity w. Various investigations by other workers (ref. 47, 48) have indicated that the contact surface, despite deceleration of the shock front, moves at an almost constant speed which is determined by the initial shock velocity. The first expansion signal finally enters the quiescent gas behind the reflected shock and changes the conditions at the observation windows.

In the case of faster shock waves, it is not the expansion fan but the wave produced by refraction of the reflected shock at the interface which disturbes the observation. The shock tube was dimensioned so that an observation time of at least 1 msec is possible throughout the projected range of Mach numbers..

It was calculated (ref. 49) that the aluminum tube with a wall thickness of 10 mm would withstand 110 atm. under static conditions. Because of shock stress, it is suitable to admit shock waves which produce only half of this value, viz. 55 atm. behind the reflected shock. Steel flanges were screwed onto the aluminum pipe. The flange thicknesses and screw threads were designed to conform with these stress requirements. The main limitations in using shocks of this strength lie in the instability of the building.

Previous experiments had shown that the behavior of untreated aluminum is not any different than that of eloxized aluminum in contact with hydrazine as far as catalytic decomposition or adsorption is concerned (see p.47). Hence, this tube has not been subject to an eloxization process.

III. ACCESSORIES

Two special valves were constructed which permit an adequate rate for pumping and gas intake, resp. and which, at the same time, close tightly to withstand the pressures behind the shock waves . Another requirement was that they would consist of inert materials, such as aluminum and Teflon in order to preclude any catalytic effect upon the heterogeneous decomposition of hydrazine.

Fig. 20 shows the pumping valve. Its internal diameter when opened is not less than 18 mm so that the tube can be evacuated rapidly. When closed, the plunger is flush with the internal walls of the shock tube. The seal is provided by a Teflon O-ring and proved to be sufficiently vacuum tight. Any leak possibilities from the atmosphere have been excluded by using tombac bellows to connect the screw handle with the plunger.

Use of tombac bellows is not permissible for connecting the movable parts of the inlet valve with the outside, since N_2H_4 reacts spontaneously with copper alloys. A Teflon diaphragm fulfils the same purpose and was shown to be hermetically sealed when fixed in the way illustrated in fig. 21. All metal parts which come into contact with hydrazine are made of aluminum.

A solenoid-operated needle was installed in the axis of the tube so that the diaphragm could be ruptured by remote control (fig.19). The needle which is 4 mm in diameter, consists of a front section made of an unmagnetic metal such as brass and a rear section made of iron. An electric magnet of about 8500 coils surrounds the front section. Upon application of a d. c. pulse of about 1 amp. the iron section of the needle is pulled into the magnet and the

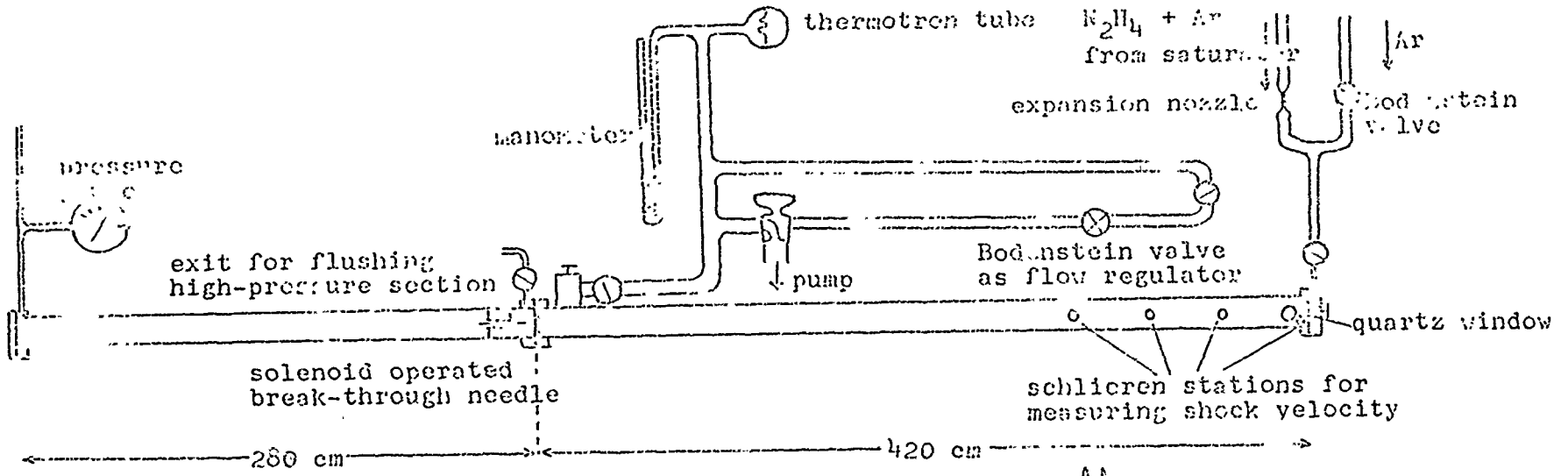

Fig. 18

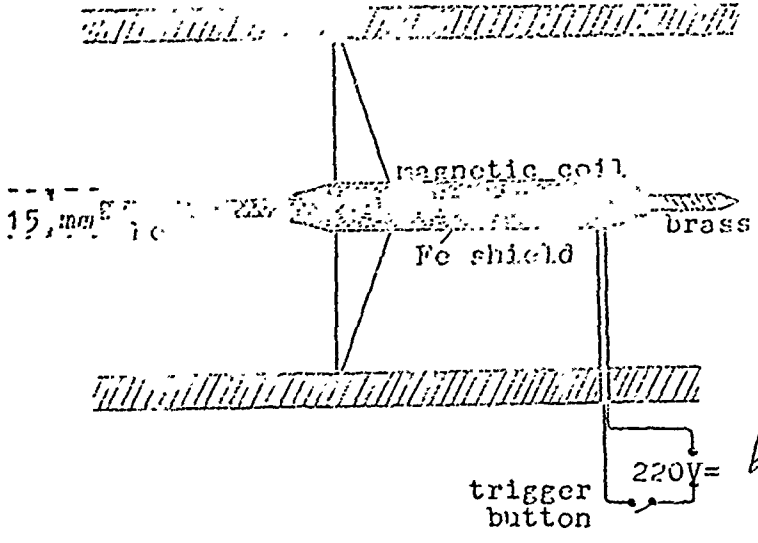

Fig. 19

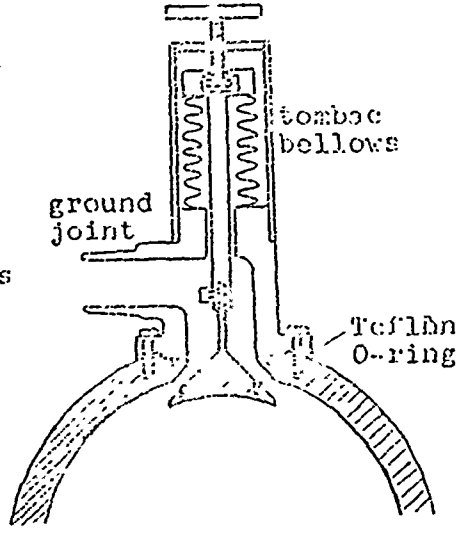

Fig. 20

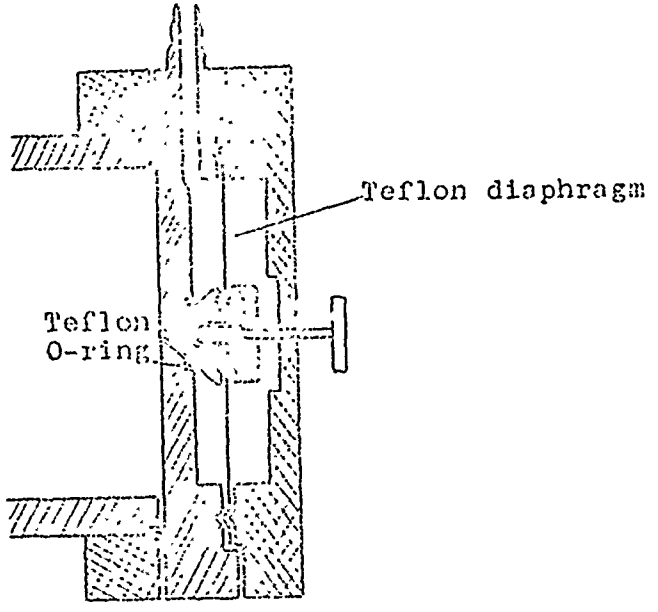

Fig. 21

brass tip breaks the diaphragm, which is strained by the driver gas nearly to its bursting pressure. The whole device, including the iron shield for the magnet has a diameter of only 15 mm (restricting the cross-section of the high-pressure part by some 2 %) and is streamlined so that no serious disturbance of the gas flow is to be expected.

A schematic sketch of the whole set-up is given in fig. 18. It has been shown (ref. 7) to be necessary to flush hydrazine containing test gases through the low-pressure section under the initial pressure of a run until adsorption equilibrium between the aluminum walls and the gas phase is attained. Then both inlet and outlet stopcocks are closed simultaneously. In order to facilitate a one-man operation, a special pumping line has been installed, which can be turned off by a stop-cock situated in the neighborhoud of the inlet stopcock. BODENSTEIN-valves allow regulation of the rate of pumping and gas intake and insure hermetic insultation of the all-glass system from the atmosphere. Fast evacuation for leak testing and for removal of adsorbed material from the shock tube walls is still possible through a short wide-bore pumping line (see fig. 18).

The low pressure section is equipped with four pairs of windows, through which the shock velocity and its attenuation are measured by the schlieren method. The windows are 40 cm apart, the last one being mounted 4 cm from the reflecting plate. At a distance of 5 cm from the closed end of the low-pressure section, there are quartz windows through which the reaction is recorded spectrophotometrically. All windows are mounted flush with the inner walls of the shock tube.

IV. PROSPECTIVE EXPERIMENTS

Since deviations from ideal shock behavior increase with decreasing shock tube diameter and decreasing initial pressure of the test gas, the advantage of the new tube is clearly that it is possible to extend experiments to lower reaction pressures, possibly $p_5 < 1$ atm. This might give indications concerning the shape of the unimolecular fall-off in the decomposition of hydrazine, ammonia and nitrous oxide. The relatively small shock-front curvature allows better time resolution and gives the opportunity to observe the decline of concentration at an earlier stage of the reaction. Moreover, the longer geometric path length of the UV beam makes it possible to investigate lower concentrations of light absorbing reactant species in Ar, i.e. conditions under which the reacting system is very close to isothermal. At the same time, it is expected that combination with flash spectroscopy, which allows scanning of the whole spectrum within a few µsec, might yield further information about the intermediates of the reaction.

F. BIBLIOGRAPHY

1.) R.C. Murray and A.R. Hall, Trans. Faraday Soc. 47, 743 (1951)

2.) A.R. Hall and A.G. Wolfhard, Trans. Faraday Soc. 52, 1520 (1956)

3.) P. Gray and J.C. Lee, Seventh Symposium on Combustion, p. 61 (Butterworths, London 1959)

4.) L. de Jaegere and A. van Tiggelen, "Determination of Activation Energy and Reaction Order in Premixed Laminar Flames". Tech. Summary Report, Contract AF 61 (514)-1245 (1959)

5.) P. Gray and J.C. Lee, Fifth Symposium on Combustion, p. 692 (Reinhold, New York, 1955)

6.) "Investigation of Gaseous Detonations and Shock-Wave Experiments with Hydrazine". Contract AF 61 (514) - 1142. Tech. Summary Report no. 2 (1960)

7.) "The Pyrolysis and Oxidation of Hydrazine in Shock Tubes". Contract No. AF 61 (514)-1142. Tech. Summary Report No. 3 (1962)

8.) L.F. Audrieth and B.A. Ogg, "The Chemistry of Hydrazine" (J. Wiley, New York, 1951)

9.) H.Gg. Wagner, in "Fundamental Data Obtained from Shock-Tube Experiments". AGARDOgraph No. 41, ed. A. Ferri (Pergamon. 1961)

10.) Landolt-Börnstein, II. Band, 4. Teil, Kalorische Zustandsgrößen. (Springer, Berlin-Göttingen-Heidelberg, 1961)

11.) B. Lewis and G. von Elbe, "Combustion, Flames and Explosions of Gases" (Academic Press, New York - London, 1961)

12.) R.A. Strehlow and A. Cohen, J. Chem. Phys. 30, 257 (1959)

13.) W.G. Parker and H.G. Wolfhard, Fourth Symposium on Combustion, p. 420 (Williams and Wilkins, Baltimore, 1953)

(...) ...B. Brandt and A.I. Rozlovskii, Doklady Akad. Nauk 132. 1129 (1960)

15.) H.H. Michel and H.Gg. Wagner, Z. physik. Chem. NF 35, 392 (1962)

16.) J.P. Chesick and G.B. Kistiakowsky, J.Chem. Phys. 28, 956 (1958)

17.) H.S. Johnston, J. Chem. Phys. 19, 663 (1951)

18.) P.J. Lindars and C. Hinshelwood, Proc. Roy. Soc. A 231, 162, 178 (1955)

19.) J.H. Gill and K.J. Laidler, Can. J. Chem. 36, 1570 (1958)

20.) M.G. Reuben and J.H. Linnett, Trans. Faraday Soc. 55, 1546 (1959)

21.) F. Kaufman, W.J. Gerry and R.B. Berman, J. Chem. Phys. 25, 106 (1956)

22.) G.M. Bell, P.L. Robinson and A.B. Trenwith, J. Chem. Soc. 1957,1474

23.) L.M. Graven, J. Am. Chem. Soc. 81, 6191 (1959)

24.) J.N. Bradley and G.B. Kistiakowsky, J. Chem. Phys. 35, 256 (1961)

25.) C.P. Fenimore and G.W. Jones, J. Chem. Phys. 63, 1154 (1959)

26.) C.P. Fenimore, J. Chem. Phys. 35, 2243 (1961)

27.) A.F. Dutta, Proc. Roys. Soc. A 178, 84 (1932)

28.) I. Freedman and J.J. Daiber, J.Chem. Phys. 34, 1271 (1961)

29.) F. Kaufman and J.R. Kelso, J. Chem. Phys. 23, 602 (1955)

30.) L. Camac and A. Vaughan, J. Chem. Phys. 34, 460 (1961)

31.) J. F. Rink, H.T. Knight and R.M. Duff, J. Chem. Phys. 34, 1942 (1961)

32.) R.E. Huffman and N. Davidson, J. Am. Chem. Soc. 81, 2311 (1959)

33.) T.B. Slater, "The Theory of Unimolecular Reactions" (Cornell University Press, Ithaca, 1959)

34.) G.B. Kistiakowsky and G.G. Volpi, J. Chem. Phys. 27, 1141 (1957)

35.) J.P. Chesik and G.B. Kistiakowsky, J. Chem. Phys. 28, 956 (1958)

36.) Th. Just and H.Gg. Wagner, Z. Elektrochemie 64, 501 (1960)

37.) Th. Just, P.J. Luig and H.Gg. Wagner, Z. Elektrochemie 65, 403 (1961)

38.) Th. Just, W. Futch and H.Gg. Wagner, Z. Elektrochemie 65, 410 (1961)

39.) G. Taylor, Proc. Roy. Soc. A 200, 235 (1950)

40.) B... Kistiakowsky and P.I. Lydd, J. Chem. Phys. 23, 271 (1955)

41.) J.I. Bourgoyne, F.J. Weinberg, Proc. Roy. Soc. A 224, 286 (1954)

42.) ..C. Lin and W.I. Fyfe, Phys. Fluids 4, 242 (1961)

43.) K.L. Wray, J. Chem. Phys. 37, 1254 (1962)

44.) .. Ivance, Proc. Roy. Soc. A 198, 267 (1949)

45.) B.. Greene and J.P. Toennies, "Chemische Reaktionen in Stoßwellen" (B. Steinkopff Verlag, Darmstadt, 1959)

46.) J.N. Bradley, "Shock Waves in Chemistry and Physics" (J. Wiley, New York, 1962)

47.) J.P. Toennies and B.P. Greene, J. Chem. Phys. 26, 655 (1957)

48.) ..L. Duff, Phys. Fluids 2, 207 (1959)

49.) DK 621.642.02, AD-Merkblatt B 1, Berechnung von Druckbehältern August 1959.